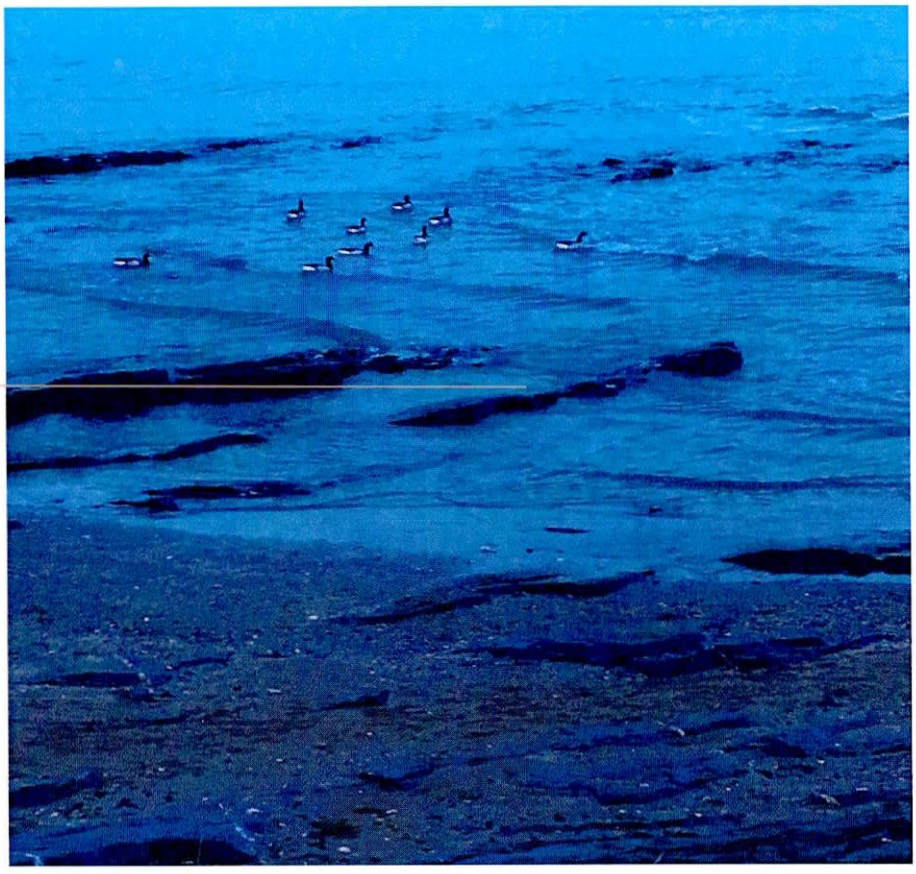

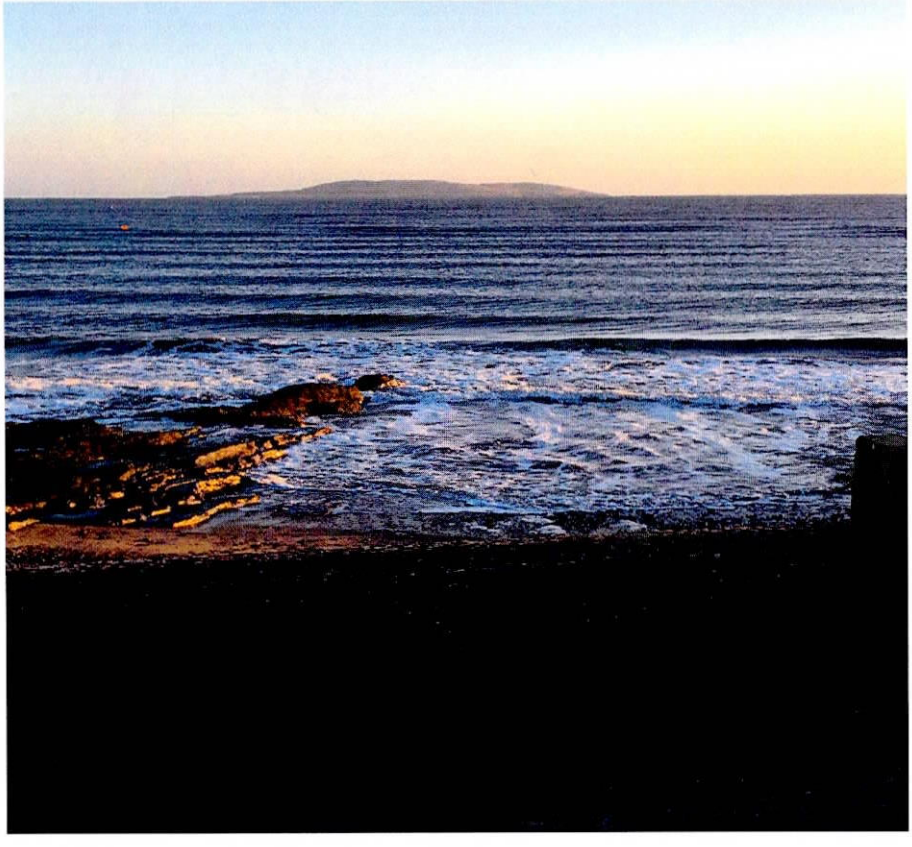

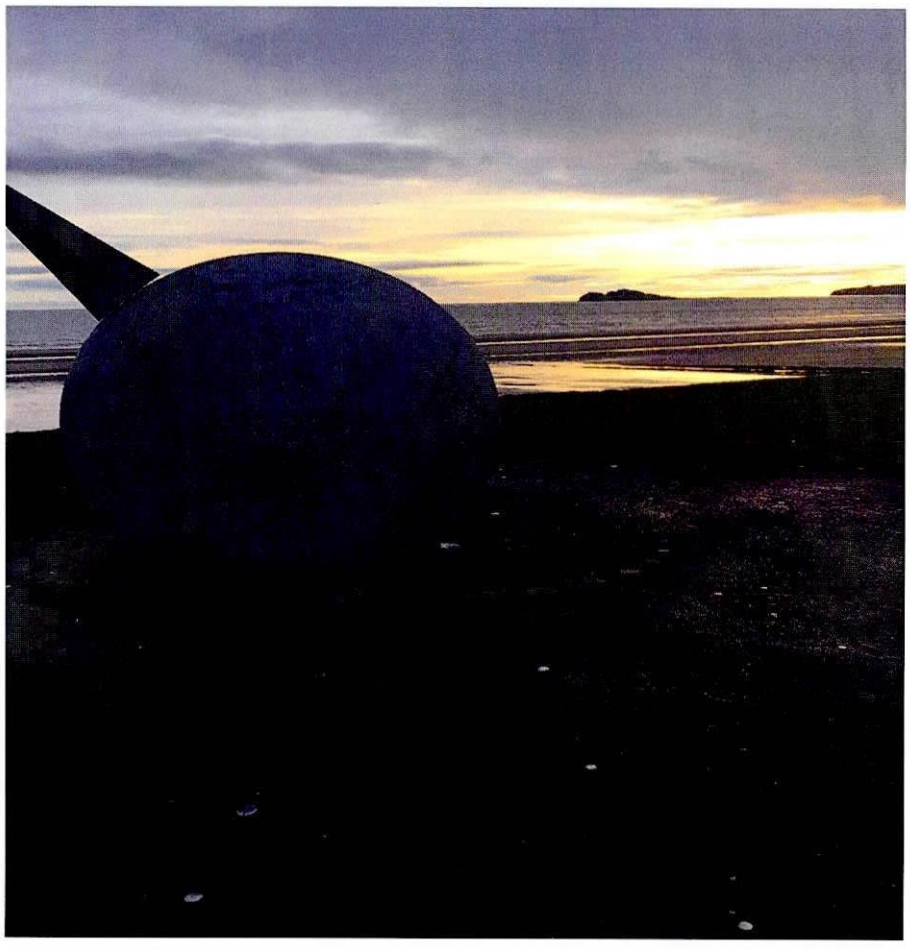

North American Society for Trenchless Technology (NASTT)
NASTT's 2014 No-Dig Show

Orlando, Florida
April 13-17, 2014

MM-T5-02

Salvaging the Lessons Learned from a Difficult Microtunneling Project

Kimberlie Staheli, Ph.D., P.E., Staheli Trenchless Consultants, Seattle, WA
Peter Robertson, Ph.D., P.E., Gregg Drilling and Testing, Huntington Beach, CA
Paul Vadnais, Vadnais Corporation, San Diego, CA
Dylan Davidson, Staheli Trenchless Consultants, Seattle, WA

1. ABSTRACT

When a trenchless project fails it is bad for everyone involved on the project- the Owner, Designer, and Contractor. However, it is also bad for the entire trenchless industry. For the industry to move forward in a positive direction, we must take a hard look at project failures to determine why the project failed so that we can use the lessons learned to eliminate repeat failures. This paper details a forensic analysis of a failed microtunneling project that appeared to be ideal for the technology at the time of design. However, as the project was constructed, a unique set of circumstances, all of which could have been avoided with proper design and execution, resulted in project failure that included loss of line and grade to the extent that the pipe would not flow by gravity, flooded shafts, and broken jacking pipe. The paper presents the geotechnical conditions that were understood to exist at the time of construction, the details of the microtunnel construction, and the resulting microtunneling failure. The results of the forensic analysis will then be presented, including post-construction geotechnical work that was performed to determine the cause of failure. The lessons learned from the design and construction will be presented along with suggestions on how to prevent similar problems on future microtunneling projects. The lessons from this project will benefit the microtunneling design and construction industry.

2. INTRODUCTION

A large construction project was planned in California very near the Pacific Coast. The project included the construction of a new pump station that would replace a number of smaller lift stations. As part of the project, a new 24-inch microtunnel was designed at a very flat grade to carry sewage from a to-be-decommissioned lift station to the new lift station that was constructed as part of the project. The microtunnel was to be constructed in eight drives within a very sensitive wetland and would traverse beneath an environmentally sensitive inter-coastal canal. The authors of this paper were hired to analyze the project after the completion of five drives, at which point the Owner terminated the construction of the microtunnels. The project then proceeded into litigation which has subsequently been settled. Due to the sensitive nature of the issues, the names of the Owner, Project, and Designer are not presented in this paper.

3. DESIGN OF THE PROJECT

The project included the construction of a new lift station, followed by a series of eight microtunnels totaling 3,445 feet in length. The drives ranged in length from 316 feet to 581 feet. Drive 1 of the microtunnel project was to use

the wet well of the lift station as a reception shaft, and the following seven drives were to move away from the lift station toward the Pacific Ocean, as can be seen in Figure 1. Of critical importance was Drive 6, which was to traverse beneath a channel within a critical wetland area with less than three feet of cover above the crown of the pipe on a very flat grade of 0.1%.

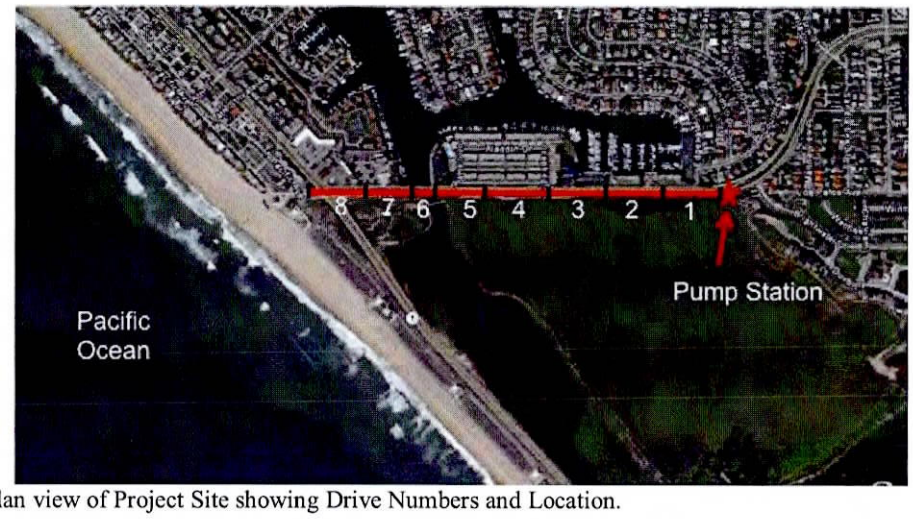

Figure 1. Plan view of Project Site showing Drive Numbers and Location.

The microtunnel project designers hired a geotechnical engineering firm to conduct a geotechnical investigation for the microtunnel design. Ten geotechnical borings were conducted along the microtunnel alignment, generally at the shaft locations, averaging one boring every 344 feet. The borings collected information on the soils to be encountered at the site. The geotechnical investigation revealed that the site soils consisted of layers of sand, silt, and clay. During the geotechnical investigation groundwater was discovered within 10 feet of the ground surface; however, no piezometers were installed during the design to track the groundwater levels or fluctuations in groundwater elevations during the design of the project.

The design documents allowed the Contractor to select between using vitrified clay pipe (VCP), Hobas, or Polycrete pipe material for the construction of the 24-inch microtunnel pipeline.

The design allowed the Contractor to select the type of shafts from a list provided in the specification. The list included sheet piles with internal bracing (although at some location the use of vibratory hammers was prohibited), corrugated metal pipe within a drilled shaft, interlocking grout columns (or secant piles), and interlocking soil-mixed columns. Although a geotechnical baseline report was not prepared for the project, the design documents listed each shaft by station and baselined the amount of fill that would be encountered at each shaft location. As the shafts were temporary shoring, the responsibility of the design was left to the Contractor.

The design required the microtunneling to begin at Drive 6 (the drive that traversed beneath the channel with minimal depth of cover); however, the design gave no information as to why the microtunnel had to start at this location.

Of interest in the design, the specification set a minimum depth of cover requirement for the microtunnel that was equal to two diameters or six feet; however, the drive beneath the channel had only 2.6 feet of cover over the crown of the tunnel. Another significant feature of the specifications that would play a large role in later litigation was that the specification required the Contractor to calculate the buoyancy of the pipeline and submit the calculations. Although all of the designed pipe options were buoyant under the design conditions, they were buried sufficiently deep to prevent flotation of the pipelines.

4. CONSTRUCTION OF THE PROJECT

Construction of the project began with the lift station. The Contractor began with a massive dewatering effort to lower the water table and allow the construction of the lift station; however, they encountered pressurized water in what was thought to be the Talbert aquifer which was known to exist beneath the site. The Owner acknowledged the existence of the pressurized aquifer and paid a sizeable change order to the Contractor to depressurize the aquifer to allow the construction. All of this activity took place prior to the construction of the microtunnel. Although the microtunneling contractor was referred to the geotechnical report for the lift station in the bidding documents, none of the information regarding the pressurized aquifer or the change order that was executed on the lift station contract was incorporated into the geotechnical documents or given to the microtunneling contractor during bidding or at any time during the construction.

The low bid contractor was awarded the microtunneling contract as the lift station was approaching completion. The Contractor elected to install 24-inch VCP with a 31-inch outer diameter (OD). The Contractor used a 30-inch Iseki Unclemole for the construction of the microtunnels. Shaft construction was completed using corrugated metal pipe with the drilled shaft method. Shaft construction began closest to the Lift Station and progressed toward the Pacific Ocean. Because the lift station wet well was approaching completion, the Contractor submitted an RFI asking if they could install Drive 1 first, microtunneling from Drive Shaft 2 to the lift station. Although the contract required Drive 6 to be installed first, the Construction Management team allowed the Contractor to proceed with the drive closest to the lift station first.

5. MICROTUNNEL DRIVES

Drive 1 was constructed in the month of October, and the 391-foot drive was completed without issue. The drive record showed that the pipe was installed within ½ -inch of line and grade. Line and grade tolerance was specified as +/- 1-inch of line and grade so the drive was installed well within the required tolerance. The machine was retrieved within the lift station wet well. Figure 2 shows the position of the laser relative to the target within the 24-inch machine during construction of Drive 1.

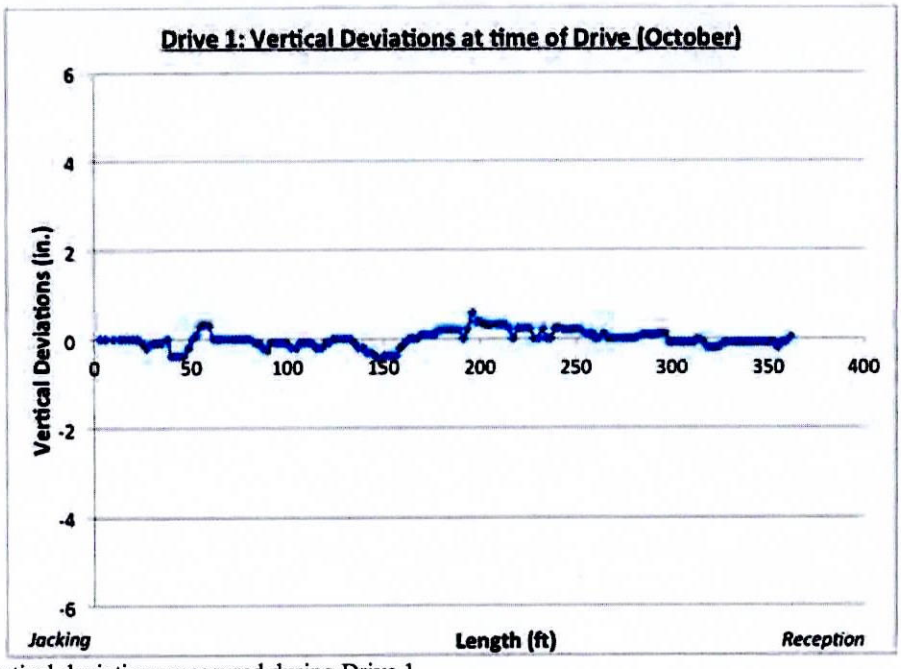

Figure 2. Vertical deviations measured during Drive 1.

After retrieval of the machine, the Contractor turned the machine within the shaft and started Drive 2 – the 524-foot drive toward the Pacific Ocean. This drive was constructed in the month of November and the vast majority of the

drive was completed within ¼ of an inch of the design line and grade. At one location the grade was ½-inch low, which was the largest deviation from line and grade on the entire drive. Figure 3 shows the location of the laser relative to the target located in the 24-inch microtunneling machine.

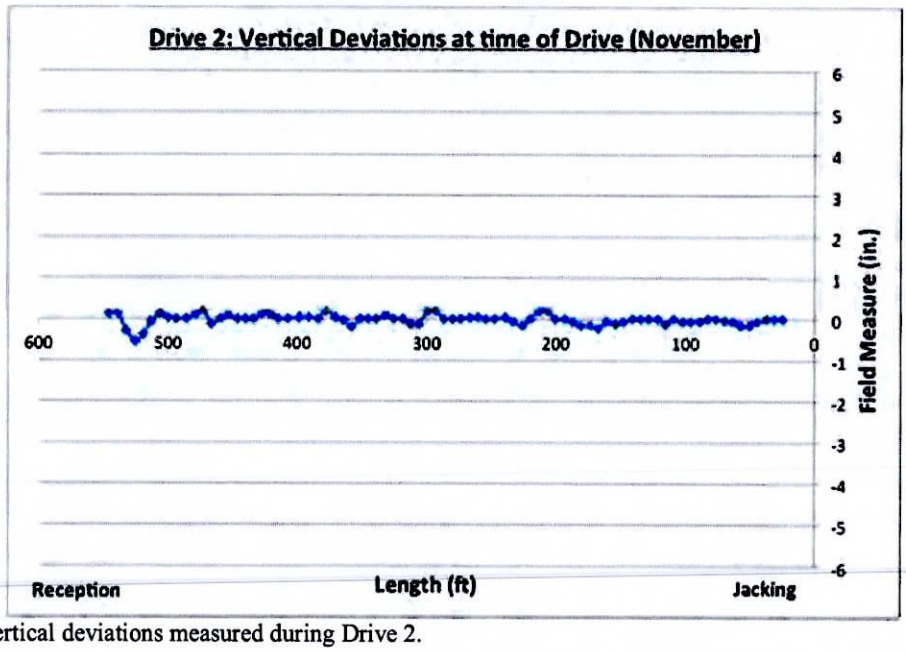

Figure 3. Vertical deviations measured during Drive 2.

In January of the following year, the Contractor moved the microtunneling equipment to the next jacking shaft to begin Drive 3, a 444-foot drive towards Drive 2. During the drive, the operator noted grade deviations of up to one inch at 110 feet and 220 feet into the alignment and was forced to move the laser to keep the laser on the target within the 24-inch machine. While pushing within 50 tons of the safe jacking capacity of the pipe (calculated with a safety factor of 2.5), the pipe broke at 460 feet into the drive. The breakage of the pipe was significant and allowed water to flow within the pipe. This water flooded the machine and the shaft, causing numerous problems and a significant delay. The microtunnel machine required retrieval from the surface and Drive 3 had to be completed by open cut excavation. Figure 4 shows the location of the laser relative to the target in the 30-inch microtunneling machine prior to the time the pipe broke and the drive was abandoned.

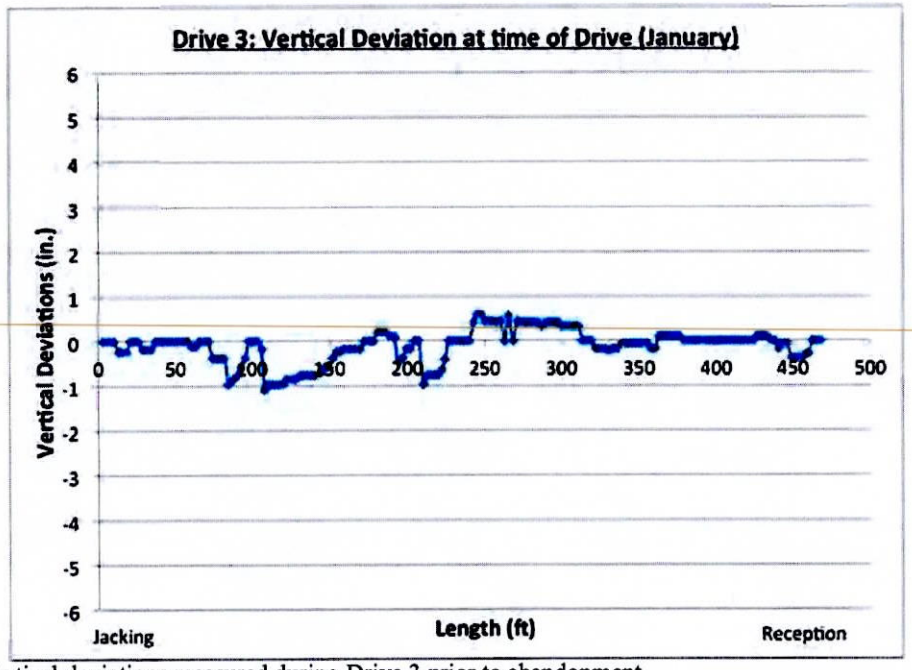

Figure 4. Vertical deviations measured during Drive 3 prior to abandonment.

Drive 4 began in April, at which time the Contractor rotated the equipment in the shaft and began the 316-foot drive toward the Pacific Ocean. The drive was completed with little incident and was completed successfully with less than ½-inch deviation on line and grade. Figure 5 shows the location of the laser relative to the target within the 30-inch machine during the drive.

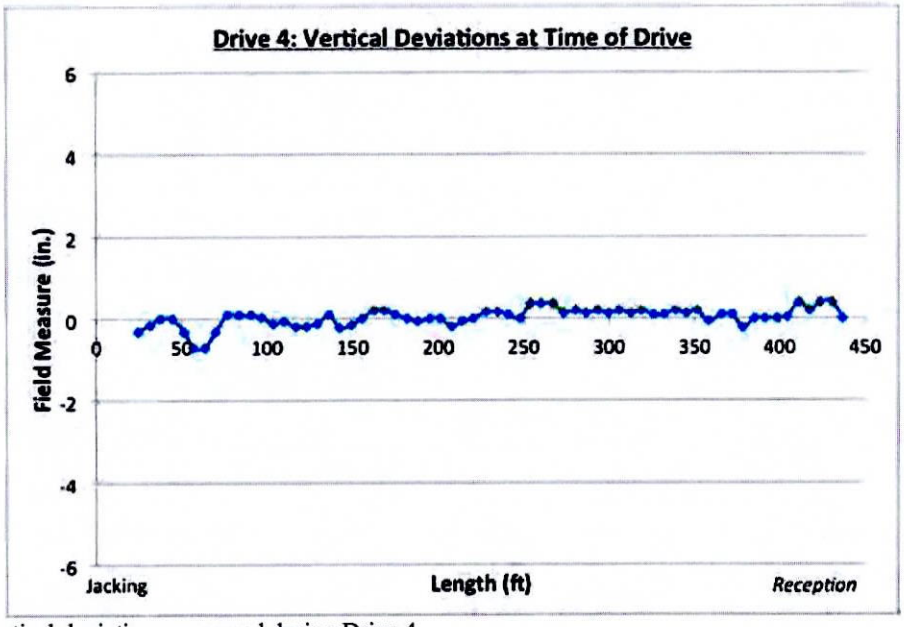

Figure 5. Vertical deviations measured during Drive 4.

For Drive 5, the Contractor relocated the equipment to the next jacking shaft and began the 445-foot drive towards Drive No. 4. This drive marked the beginning of a series of perplexing events that would ultimately result in the failure of the entire project. The drive began without incident and had progressed for approximately 300-feet when

grade deviations in the pipe were noted at the pipes near the shaft. When these pipes were initially installed by the microtunnel machine, the microtunneling equipment guidance system showed that they were within the one inch line and grade tolerance; however, as the drive progressed, the pipes were beginning to increase in grade. This trend continued as the drive extended, as the pipes within 150 feet of the shaft rose upward and caused a hump in the pipe that deviated by as much as 13 inches from line and grade. The drive was finished with the machine at the appropriate line and grade; however, the 13-inch hump in the pipe was significant and would not allow the sewage to flow by gravity to the Lift Station. Figure 6 shows the grade deviations of the pipe as it was being constructed (i.e. the position of the laser relative to the machine target), along with the as-built survey of the pipe at the completion of the tunnel drive. It is important to note that by the end of the tunneling the operator was forced to move the laser to keep it on the target due to the large hump in the pipeline. These values were corrected on Figure 6 to reflect the actual position of the machine based on the operator's notes that kept track of the laser movement.

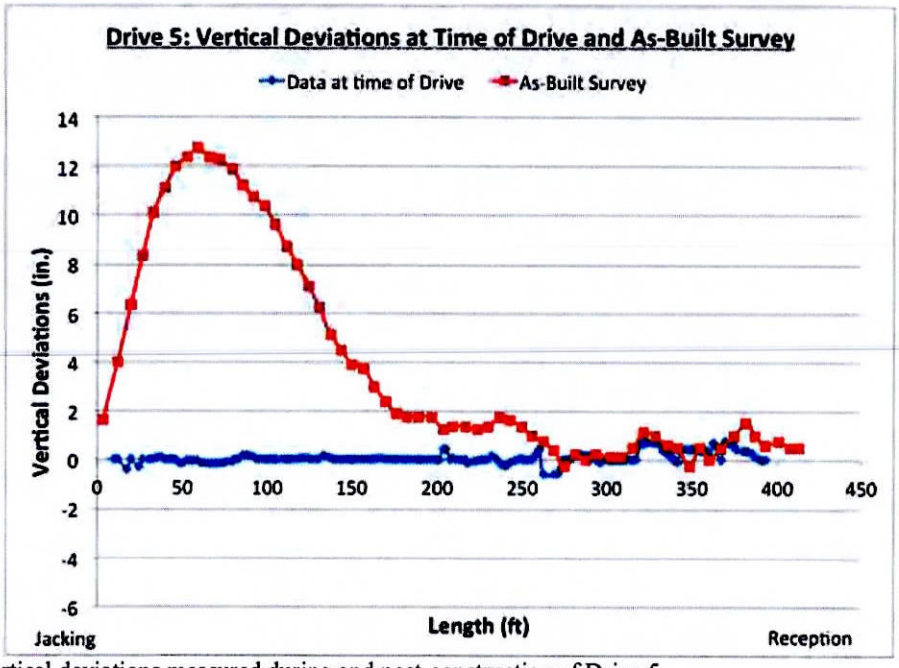

Figure 6. Vertical deviations measured during and post-construction of Drive 5.

It was unclear at this point why the pipe had risen during jacking as there was no indication of encountering an obstruction or any object that would have caused the machine to rise – in fact, the machine was on line and grade during the excavation of the first 275 feet. The rise in the pipe occurred after excavation, but the question was – why?

6. INVESTIGATING THE PROBLEM

After the pipe on Drive 5 had risen, it was decided to go back and re-survey the other microtunnel drives (1 through 4) to determine their exact locations. The results of the surveys were astonishing. Drive 1, which had originally been installed within the specified line and grade tolerance at the time of construction, had shown significant movement. In fact, there were locations where the pipe exhibited humps that were five and four inches out of tolerance, as shown in Figure 7. With the tight grades specified on the project, the areas exhibiting the deviations were significant enough that they would require repair to allow the sewer to flow by gravity.

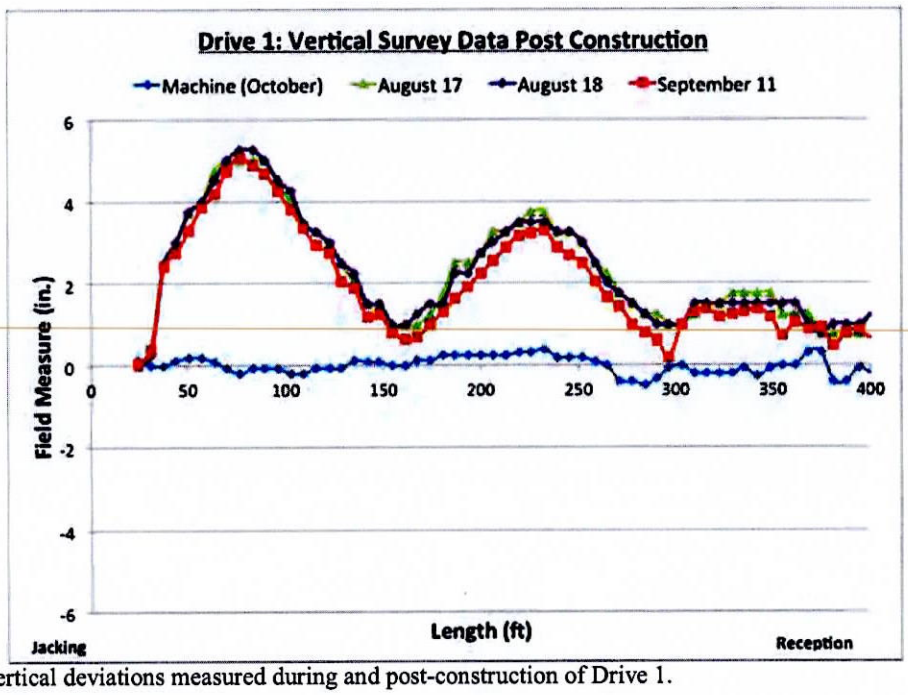

Figure 7. Vertical deviations measured during and post-construction of Drive 1.

Drive 2 was re-surveyed but showed essentially no change in grade from the original installation to the re-survey. Drive 3 could not be surveyed because it contained the as-yet unfixed broken pipe, allowing water into the excavation and making entry unsafe. When Drive 4 was re-surveyed, significant deviations in line and grade appeared, even though it had been installed within line and grade tolerances only three months prior to the re-survey. Drive 4 showed grade deviations of four-inches and two and 1/2 - inches at the near-shaft locations, as shown in Figure 8.

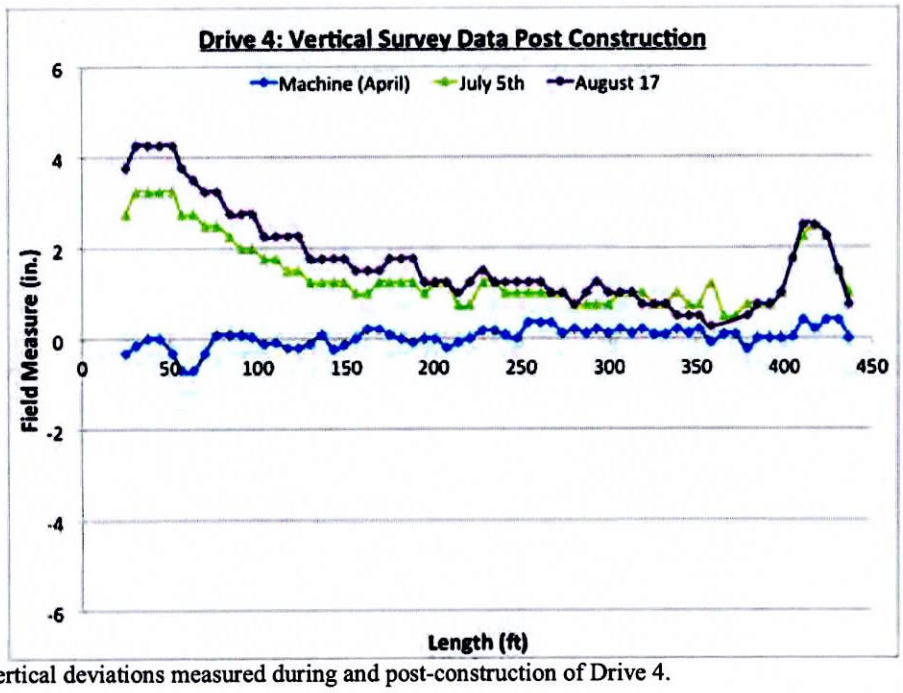

Figure 8. Vertical deviations measured during and post-construction of Drive 4.

At this point the microtunneling was stopped. There was no sense in microtunneling beneath the channel because the deviations in line and grade were of such significance that gravity flow could not be achieved in the remainder of the pipeline. In addition, the Contractor was very concerned that the machine would "daylight" within the channel due to the shallow depth of cover.

7. DETERMINING THE CAUSE OF FLOTATION

There were many theories as to the cause of flotation, several of which focused on the buoyancy of the pipe. There was no disagreement that the pipe was buoyant; however, there was disagreement over what had occurred during tunneling to cause flotation of the pipe when the depth of the pipeline was sufficient to prevent upward movement due to buoyancy forces.

Some theorized that over-excavation had taken place during microtunneling operations; however, there was no evidence of over-excavation in the jacking record. In addition, over-excavation would not have explained the flotation. In order for over-excavation to occur, the soil must be loose/soft enough to flow into the face of the machine. If this scenario exists, the soil will also collapse over the machine and subsequent pipe. If the pipe is sufficiently deep that the overburden forces are higher than the upward buoyant force of the pipe, the pipe will not float. If the soil was stiff enough to hold a competent hole, keeping the overcut open, the pipe could float by means of the upward buoyant force to the limits of the overcut; however, over-excavation would not occur because the soil would need to be sufficiently stiff to hold the overcut, and therefore collapsing of the soil into the face of the machine would not occur.

There were some that theorized that the microtunneling machine had liquefied the loose granular soils, causing flotation of the pipeline; however, liquefaction would have caused the microtunneling machine to sink. During the microtunnel drives, the microtunneling machine had no difficulty with maintaining grade and did not encounter any areas where bearing capacity of the soils beneath the machine were of any issue. In addition, the maximum rotation of the machine was eight revolutions per minute, well below the frequency that would be necessary to cause liquefaction of the soil.

To determine the cause of the flotation it was necessary to take a critical look at the geotechnical conditions along each of the drives. It was discovered early in the analysis that the Contractor for the Lift Station had encountered pressurized water during the dewatering process. Once this was discovered, monitoring well records from the local County agency were requested for analysis to determine if pressurized groundwater conditions existed historically. Those records revealed several dewatering wells within close proximity to the construction site (one well was only 256 feet from one of the microtunnel drives). The monitoring well records revealed that there were three main aquifers at the site: a shallow aquifer that contained perched water near the ground surface that was referred to as the "Shallow Aquifer System or Layer 1"; an aquifer that was below the shallow aquifer system known as the "Primary Aquifer System or Layer 2" which would become seasonally pressurized; and a third aquifer referred to as the "Deep Aquifer System or Layer 3." All of the aquifers were separated by aquitards or layers of clay. Of critical importance was Layer 2 as it was where the microtunnel was located.

The geotechnical conditions at the site were analyzed to compare the flotation of the pipe with the locations of the aquifers and the records at the monitoring wells. The geotechnical conditions for Drive 4 are shown in Figure 9. The geotechnical conditions revealed that the microtunnel was designed just below an aquitard that separated the Shallow Aquifer System and the Primary Aquifer System.

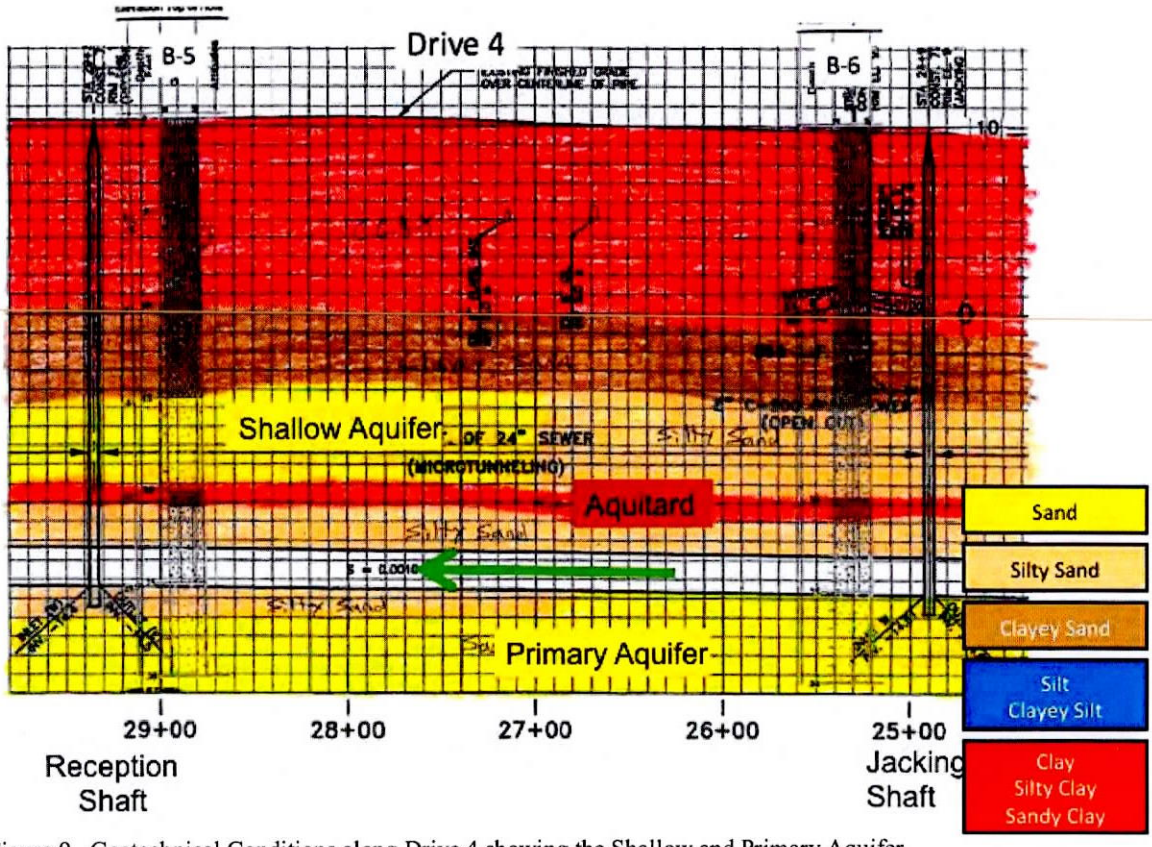

Figure 9. Geotechnical Conditions along Drive 4 showing the Shallow and Primary Aquifer.

An examination of Drive 4 revealed that at the time of construction, the water in the primary aquifer was not pressurized, according to the County monitoring wells. However, within a month after construction, the primary aquifer became pressurized and some wells exhibited artesian pressures. Figure 8 showed that the flotation effects were the highest nearest the shaft locations. It was then determined that the shafts had breached the aquitard during construction and were not completely sealed at the interface, creating a pathway between the shallow and primary aquifers. Since the pipe was designed only a few feet beneath the aquitard, the critical gradient to cause piping of the sandy soils between the shallow and primary aquifer was very low. When the pressure in the primary aquifer began to rise above that in the shallow aquifer, the water began to migrate upwards into the shallow aquifer. Nearest the shafts where the aquitard had been breached, the movement of water took soil particles with it, removing the soil from above the pipeline. Since the pipe was buoyant, the pipe floated into the space that was vacated by the soil that had moved into the shallow aquifer due to soil piping. These effects were not seen on Drive 4 during construction because the primary aquifer was not pressurized at the time of construction.

However, on Drive 5, the primary aquifer was pressurized during the time of construction. In fact, as they were microtunneling, the primary aquifer was pressurized to the point that the critical gradient was reached near the jacking shaft location. This caused the soil above the pipe to begin piping/moving above the aquitard (clay) layer during the installation of the pipe. Although the Contractor was installing the pipe to the design line and grade, the pipe began to float during the installation because of the pressure gradient between the Shallow and Primary Aquifers. Figure 10 shows the geotechnical conditions on Drive 5 during construction.

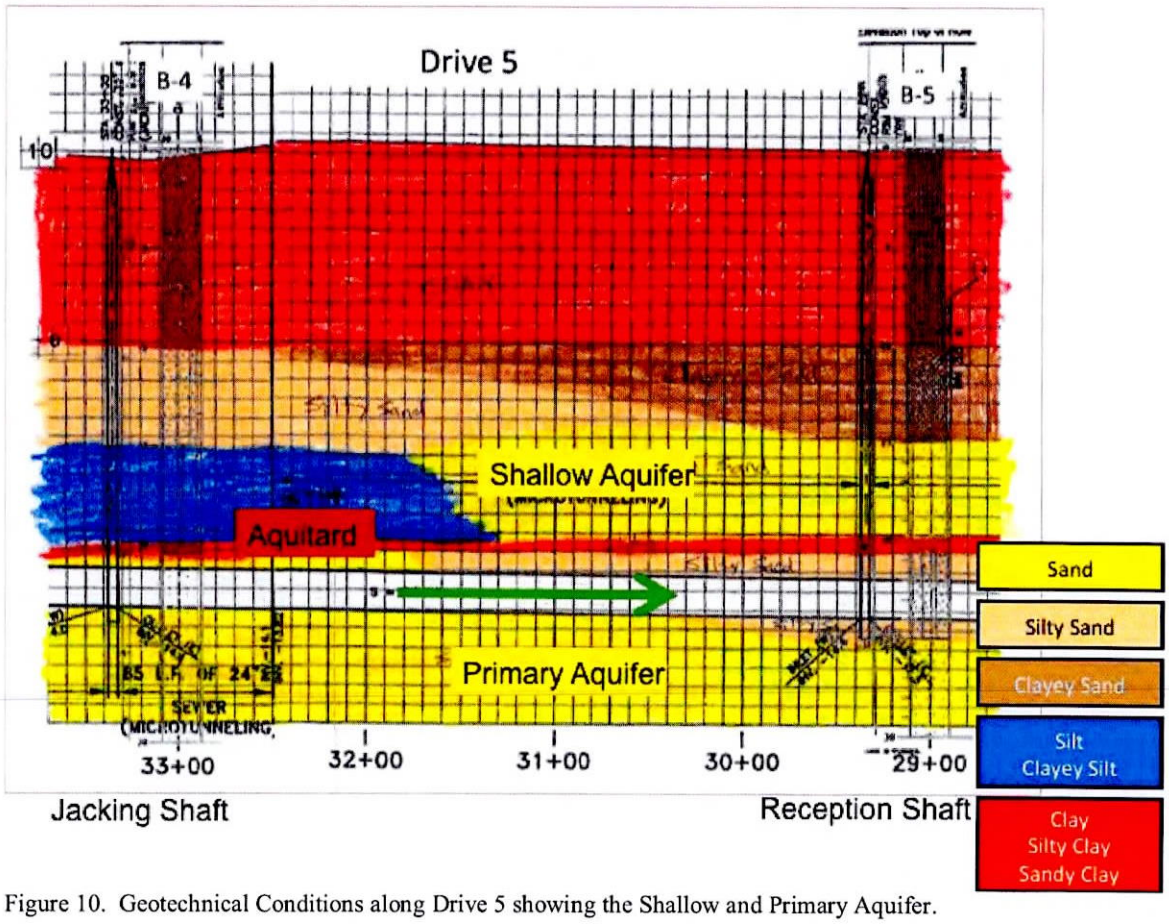

Figure 10. Geotechnical Conditions along Drive 5 showing the Shallow and Primary Aquifer.

Of note on Drive 5 was the fact that the aquitard is significantly thick in the area where the piping occurred, resulting in flotation of the pipe; however, beyond approximately 250 feet into the drive, the aquitard shrinks to less than 6 inches thick. In Boring B-5, the aquitard is seen only as a thin layer of clay, which has been interpreted to stretch along the drive. It is therefore possible that the aquitard is in fact discontinuous, allowing the pressures to equalize during tunneling, and eliminating the potential for pipe flotation in that area.

Drive 1 showed a similar pattern to Drives 4 and 5 with an aquitard within a few feet of the pipe, sandy soils above the pipe that were susceptible to piping, and flotation of the pipe near the shaft locations where the aquitard was breached by the shaft construction. However, of equal importance was Drive 2 where no flotation was observed during or post construction. The geotechnical conditions for Drive 2 are shown in Figure 11.

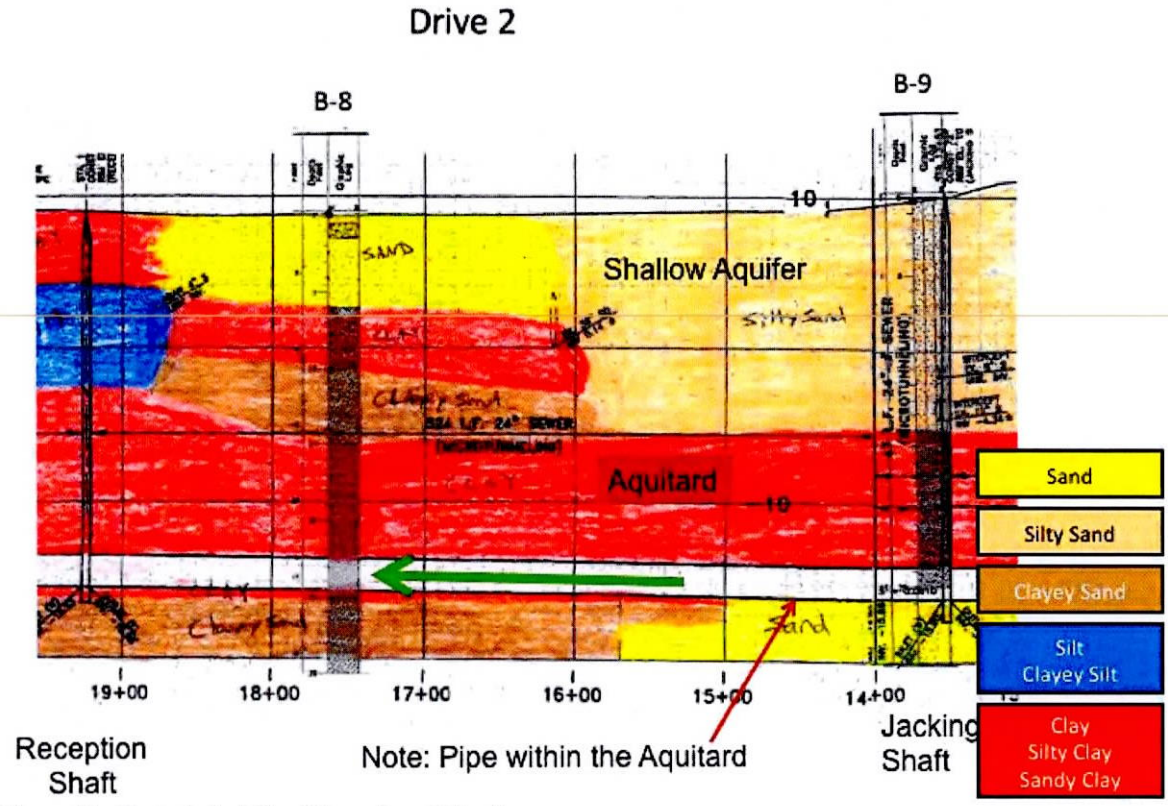

Figure 11. Geotechnical Conditions along Drive 2.

Drive 2 was constructed almost entirely within clay. At no point along the drive was there a condition where there was sand above the pipe as the alignment was completely within the clay aquitard. Because of this fact, there was no soil above the pipeline that was susceptible to piping. Although the primary aquifer became pressurized on this drive, as with all the other drives, piping of the soils did not occur as clay is not susceptible to piping under the pressure gradient that was measured in the monitoring wells. Therefore, there was no flotation of the pipeline. This proved to be the case as the post construction surveys revealed that no flotation had taken place on Drive 2 after the pressurization of the aquifers.

8. CONCLUSIONS AND LESSONS LEARNED

There were many valuable lessons learned on the project. The most prominent lesson learned was the importance of gathering groundwater information on microtunneling projects. Although it was widely known to the designers that the groundwater table was close to the ground surface at the project site (which was one of the main reasons that microtunneling was the chosen method of construction), piezometers were not installed at the site to measure the groundwater fluctuations over the course of the design. Had the designers had access to piezometer data, they surely would have seen the fluctuations in the groundwater pressures and could have changed the design accordingly.

If pressurized water was known to exist at the site, it would have been critical to include a grouting program with the shaft design to completely seal the shafts so that no piping could have occurred at the location of the shafts. Alternatively, the pipeline could have been deepened below the aquitard so that the critical gradient was much higher and would not have been reached with the water pressure fluctuations that were expected in the local area.

Another valuable lesson learned from the project was the importance of sharing information from the lift station contract with the microtunneling contract. Although this would have taken some coordination on the part of the construction management consultant and design consultant, the fact that the lift station Contractor was aware of the pressurized aquifer in the year preceding the microtunneling construction was tremendously valuable information.

Had the coordination taken place and the information been included in the microtunneling contract, it would have certainly resulted in a higher bid price for grouted shafts; however, the City would have ended up with a pipe that would not have floated and would have flowed by gravity.

Another lesson learned was that the microtunnel design utilized such a flat slope that there was absolutely no room for error. Had the lift station been deepened, even by two to three feet, it would have allowed for some deviation in the grade of the microtunnel pipe without failure of the project. It is understood that microtunneling is advertised to be accurate to within one-inch on 1,000 feet; however, conditions are not always perfect and it is often wise to incorporate some flexibility into the design to allow for some construction difficulties.

The channel crossing was never constructed; however, had it been constructed, the project may have had additional problems. With a very small amount of ground cover over the crown of the pipeline, it is likely that the machine would have day-lighted in the canal, causing a host of problems. Had this occurred, the environmental regulators on the project could have shut the project down causing significant delays. The risk of this crossing was extremely high and could have been mitigated by deepening the pipeline to the "standard rule" of two diameters of cover. This would have resulted in a slightly deeper lift station; however, this would have lowered the risk for the overall project.

This project was disastrous for the City who had never used microtunneling on a project before, and will likely never use microtunneling again. As a result, it hurt the entire microtunneling industry. The authors were hired as claim analysts to help determine the cause of loss and participate in mediation hearings and preparation for litigation. Although these stories can be "ugly," it is critically important that this industry shares our failures as well as our successes so that we can grow as an industry and learn lessons from the projects that do not go well. We applaud those who gave their permission to have this story told and respect those whose names have been omitted from this text for the sake of privacy.

Microb Genom. 2017 July 3(7): e000114.

Published online 2017 Jul 4. doi: 10.1099/mgen.0.000114

PMCID: PMC5605956

PMID: 29026655

Sharing of carbapenemase-encoding plasmids between Enterobacteriaceae in UK sewage uncovered by MinION sequencing

Catherine Ludden,[#1,2,†] Sandra Reuter,[#3,†] Kim Judge,[#2,3,†] Theodore Gouliouris,[#3,4,†] Beth Blane,[3] Francesc Coll,[1,2] Plamena Naydenova,[3] Martin Hunt,[2] Alan Tracey,[2] Katie L. Hopkins,[5] Nicholas M. Brown,[4] Neil Woodford,[5] Julian Parkhill,[2] and Sharon J. Peacock [1]

Author information Article notes Copyright and License information Disclaimer

Associated Data

Supplementary Materials

Abstract

Go to:

Abbreviations

AMRHAI, antimicrobial resistance and healthcare-associated infections; CPE, carbapenemase-producing Enterobacteriaceae; CUH, Cambridge University Hospitals NHS Foundation Trust; ENA, European Nucleotide Archive; IS, insertion sequence; MIC, minimum inhibitory concentration; MβL, metallo-β-lactamase; PacBio, Pacific BioSciences RSII system; SNP, single-nucleotide polymorphism; WGS, whole-genome sequencing.

Go to:

Data Summary

1. Illumina sequence data have been deposited in the European Nucleotide Archive (ENA); individual sample accession numbers are as listed in Table 1. MinION sequence data have been deposited in ENA; accession numbers: ERS634378, ERS634376 and ERS1033541 (www.ebi.ac.uk/ena/data/view/ERS634378, www.ebi.ac.uk/ena/data/view/ERS634376, www.ebi.ac.uk/ena/data/view/ERS1033541).

Table 1.

CPE isolated from wastewater and their antimicrobial-resistance mechanisms

						Genetic mechanisms derived from sequence data			
Wastewater treatment plant	**Untreated or treated sample**	**Isolate ID**	**Accession no.**	**Species**	**Phenotypic carbapenem-resistance mechanism**	**Carbapenem resistance***	**Extended-spectrum β-lactamases**	**Narrow-spectrum β-lactamases**	**Other resistance genes**
W1	Treated	VRES0316	ERS634377	*Escherichia coli*	MβL	*bla*NDM-5	–	–	Macrolide (*mphA*); sulphonamide (*sul1*); trimethoprim (*dfrA12*)
W2	Untreated	VRES0375	ERS634381	*Klebsiella pneumoniae*	MβL	*bla*NDM-1-like	–	*bla*TEM-1, *bla*OXA-1, *bla*LE	Aminoglycoside [*aac(6')-Ib-cr*, *aac(3)-*

						Genetic mechanisms derived from sequence data			
Wastewater treatment plant	**Untreated or treated sample**	**Isolate ID**	**Accession no.**	**Species**	**Phenotypic carbapenem-resistance mechanism**	**Carbapenem resistance***	**Extended-spectrum β-lactamases**	**Narrow-spectrum β-lactamases**	**Other resistance genes**
								N-25-like*	*IIa, strA/B*]; chloramphenicol (*catA1*); fosfomycin (*fosA*); quinolone (*oqxA, oqxB, qnrB1*); sulphonamide (*sul1*); tetracycline [*tet*(A)]; trimethoprim (*dfrA12, dfrA14*)
W2	Untreat	VRES0	ERS8086	*Enterobacter*	MβL	bla_{IMP-1}	–	–	Aminoglycoside

						Genetic mechanisms derived from sequence data			
Wastewater treatment plant	**Untreated or treated sample**	**Isolate ID**	**Accession no.**	**Species**	**Phenotypic carbapenem-resistance mechanism**	**Carbapenem resistance***	**Extended-spectrum β-lactamases**	**Narrow-spectrum β-lactamases**	**Other resistance genes**
	ed	377	29	*cloacae*complex					(*aac(6')-Ib*, *aadB*); fosfomycin (*fosA*); macrolide (*ereA*); quinolone (*qnrA1*); sulphonamide (*sul1*); trimethoprim (*dfrA1*)
W2	Untreated	VRES0379	ERS8086030	*Klebsiella oxytoca*	OXA-48-like	*bla*$_{OXA-48}$	*bla*$_{CTX-M-15}$, *bla*$_{OXY-6}$	*bla*$_{TEM-1}$, *bla*$_{OXA-1}$	Aminoglycoside [*aac(6')-Ib-cr*, *aac(3')-IIa*, *strA*, *strB*]; trimethopri

						Genetic mechanisms derived from sequence data			
Wastewater treatment plant	**Untreated or treated sample**	**Isolate ID**	**Accession no.**	**Species**	**Phenotypic carbapenem-resistance mechanism**	**Carbapenem resistance***	**Extended-spectrum β-lactamases**	**Narrow-spectrum β-lactamases**	**Other resistance genes**
									m (*dfrA14*); quinolone (*qnrB1*); sulphonamide (*sul2*); tetracycline [*tet*(A)]
W3	Untreated	VRES0380	ERS634382	*Klebsiella pneumoniae*	OXA-48-like	*bla*OXA-181 and *ompF*†	*bla*CTX-M-15, *bla*SHV-12, *bla*CMY-4	*bla*TEM-1	Aminoglycoside [*aac(6')-Ib-cr, armA*]; fosfomycin (*fosA*); macrolide (*ermB, mphE, msrE*); quinolone (*oqxA,*

						Genetic mechanisms derived from sequence data			
Wastewater treatment plant	**Untreated or treated sample**	**Isolate ID**	**Accession no.**	**Species**	**Phenotypic carbapenem-resistance mechanism**	**Carbapenem resistance***	**Extended-spectrum β-lactamases**	**Narrow-spectrum β-lactamases**	**Other resistance genes**
									qnrS1); rifampicin (*arr-2*); sulphonamide (*sul1*); trimethoprim (*dfrA12*)
W4	Untreated	VRES0269	ERS634376	*Raoultella ornithinolytica*	OXA-48-like	*bla*$_{OXA-48}$	*bla*$_{SHV-12}$	*bla*$_{TEM-1}$	Aminoglycoside [*aac(6')-Ib, aac(6')-IIc*]; fosfomycin (*fosA*); quinolone (*qnrA1*); rifampicin (*arr*); sulphonami

						Genetic mechanisms derived from sequence data			
Wastewater treatment plant	**Untreated or treated sample**	**Isolate ID**	**Accession no.**	**Species**	**Phenotypic carbapenem-resistance mechanism**	**Carbapenem resistance***	**Extended-spectrum β-lactamases**	**Narrow-spectrum β-lactamases**	**Other resistance genes**
									de (*sul1*, *sul2*)
W4	Untreated	VRES0273	ERS634378	*Enterobacter kobei*	OXA-48-like	bla_{OXA-48} and *ompCF*‡	bla_{SHV-12}	bla_{TEM-1}	Aminoglycoside [*aac(6')-IIc*]; fosfomycin (*fosA16*); quinolone (*qnrA1*); rifampicin (*arr*); sulphonamide (*sul1*, *sul2*)
W4	Treated	VRES0	ERS1033	*Raoultella ornithinolyt*	OXA-48-	bla_{OXA-48}	bla_{SHV-12}, *blao*	bla_{TEM-1}	Aminoglycoside

						Genetic mechanisms derived from sequence data			
Wastewater treatment plant	**Untreated or treated sample**	**Isolate ID**	**Accession no.**	**Species**	**Phenotypic carbapenem-resistance mechanism**	**Carbapenem resistance***	**Extended-spectrum β-lactamases**	**Narrow-spectrum β-lactamases**	**Other resistance genes**
		259	541	*ica*	like		XA-17		[*aac(6')-Ib*, *aac(6')-IIc*]; fosfomycin (*fosA*); quinolone (*qnrA1*); rifampicin (*arr*); sulphonamide (*sul1*, *sul2*)
Cambridge hospital sewer	Untreated	VRES0183	ERS634380	*Klebsiella pneumoniae*	KPC	*bla*GES-s and *ompCF§*	*bla*CTX-M-15, *bla*SHV-12	*bla*OXA-1, *bla*TEM-1	Aminoglycoside [*aac(6')-Ib*, *aac(6')-Ib-cr*, *aac(3)-IIa*, *aph(3)-*

					Genetic mechanisms derived from sequence data				
Wastewater treatment plant	**Untreated or treated sample**	**Isolate ID**	**Accession no.**	**Species**	**Phenotypic carbapenem-resistance mechanism**	**Carbapenem resistance***	**Extended-spectrum β-lactamases**	**Narrow-spectrum β-lactamases**	**Other resistance genes**
									Ia]; fosfomycin (*fosA*); macrolide (*mphA*); quinolone (*oqxA*, *oqxB*); tetracycline [*tet*(A), *tet*(D)]

Open in a separate window

*Genes labelled as '-like' differ from the named gene by 1 aa change.

†VRES0380 – *ompF* frameshift mutation.

‡VRES0273 – *ompC* insertion of IS element, *ompF* introduction of stop codon.

§VRES0183 – *ompC* introduction of stop codon and potentially IS element insertion, *ompF* frameshift mutation.

2. Supporting data, including assemblies and the fast52fastq.py script, are available from a GitHub repository (https://github.com/kim-judge/wastewater).

3. The manually finished genome of *Enterobacter kobei* has been deposited in ENA under accession numbers: FKLS01000001-

FKLS01000010 (www.ebi.ac.uk/ena/data/view/FKLS01000001 – www.ebi.ac.uk/ena/data/view/FKLS01000010).

Go to:

Impact Statement

The spread of carbapenem resistance among pathogenic Gram-negative bacilli is a major public-health threat. Studies to date have emphasized this problem in the clinical setting, largely ignoring the importance of environmental contamination and the significance of a One Health approach. The use of Illumina whole-genome sequencing to identify the genetic basis for resistance led to the discovery that several species from the same treatment plant carried the same carbapenem-resistance gene. Using the Oxford Nanopore MinION, we demonstrated putative sharing of several plasmids between different Enterobacteriaceae species (*Enterobacter kobei* and *Raoultella ornithinolytica*) in wastewater, with one plasmid carrying a carbapenemase gene conferring resistance to the carbapenem drugs, and the other containing resistance genes to numerous other drugs and heavy metals. To our knowledge, this is the first report of carbapenemase-producing Enterobacteriaceae being recovered from wastewater at UK sewage treatment plants. Importantly, we show that treatment plants do not prevent the release of these bacteria into the environment and this may provide a point of intervention. We also demonstrate the utility of a next-generation sequencing instrument, the MinION, to confirm the sharing of plasmids between bacterial isolates in wastewater, and have generated a complete genome sequence for *Enterobacter kobei*. The ease of use of this instrument would facilitate its implementation in future intervention studies that target environmental contamination with carbapenem-resistance genes.

Go to:

Introduction

The global rise of carbapenemase-producing Enterobacteriaceae (CPE) over the last decade represents a major threat to public health [1–3]. CPE are often resistant to several additional classes of antibiotics, which may limit therapeutic options to drugs with a higher toxicity profile. Unsurprisingly, invasive infections caused by CPE are associated with poor clinical outcomes and carry an excess attributable mortality compared with those caused by carbapenem-susceptible isolates [4–6]. CPE are predominantly isolated in healthcare settings, but their spread to healthy humans, livestock and the environment has been reported [4, 7]. The development of interventions that prevent further CPE dissemination requires delineation of their reservoirs and routes of spread, combined with accurate characterization of the mobile elements that transfer carbapenemase genes within and between bacterial species.

High-throughput whole-genome sequencing (WGS) has provided major insights into pathogen transmission and outbreak investigation based on core-genome phylogenetic analyses [8], but has not reached its potential to provide detailed characterization of plasmids and their transmission within specific environments.

This is due to a methodological limitation of short-read data generated by Illumina technology, from which plasmids cannot be accurately assembled because of the presence of numerous repetitive regions. Technologies including the Pacific BioSciences RSII system (PacBio) and the Oxford Nanopore Technologies MinION system generate long-read data that can overcome this barrier. It has been demonstrated previously that PacBio long-read sequencing can be successfully used to elucidate transfer of carbapenem-resistance-carrying plasmids within hospital environments [9, 10], and after years of on-going development the pocket-sized MinION is approaching a level of accuracy and usability at which it could be used to explore the central question of plasmid transmission. It has been used previously to detect the presence of antimicrobial-resistance genes and to track the transmission of viral outbreaks [11–14].

Our aim here was to apply the MinION and Illumina platforms to seek evidence for sharing of carbapenemase-encoding plasmids between bacterial species in human sewage. This reservoir contains a diversity of pathogenic and non-pathogenic bacteria that can exchange DNA (including genes encoding antimicrobial resistance) by horizontal gene transfer. CPE have been isolated from human sewage at wastewater treatment plants in Austria, Germany and Brazil, and from rivers and lakes in Switzerland, Portugal, Brazil and Vietnam [15–22], and carbapenemase-encoding plasmids have been found in wastewater in Germany [21], but definitive evidence of plasmid sharing and putative transmission is lacking.

Go to:

Methods

Wastewater processing and bacterial identification

Samples of treated and untreated wastewater were obtained from each of 20 treatment plants. At each sampling point, two consecutive grab samples of 0.5 l each were collected and mixed in 1 l sterile bottles containing 18 mg sodium thiosulphate (Sigma-Aldrich). A single 1 l wastewater sample was obtained from the main septic tank at the Cambridge University Hospitals NHS Foundation Trust (CUH) facility. All samples were transported to the laboratory on ice packs in the dark and processed within 12 h. One millilitre of triplicate serial tenfold dilutions, 10 ml untreated wastewater samples and 100 ml treated wastewater samples were concentrated using the filtration technique onto 0.45 µm pore size filter membranes (S-Pak; Merck Millipore). Membranes were then placed onto the surface of ESBL *Brilliance*agar (Oxoid) and incubated for 24 h at 37 °C in air. Duplicate membranes of the lowest dilution tested were also placed into tryptic soy broth with 2 mg imipenem l^{-1} and incubated for 24 h at 37 °C in air, followed by subculture of 100 µl on chromID CARBA SMART plates (bioMérieux), and ESBL *Brilliance* and cystine lactose electrolyte deficient (CLED) agar with a 10 µg imipenem disc.

At least one colony for each bacterial colony morphology type suspected to be Enterobacteriaceae based on colour were picked and speciated using matrix-assisted laser desorption/ionization-time of flight mass spectrometry (MALDI-

TOF MS; Biotyper version 3.1; Bruker Daltonics). Antimicrobial-susceptibility testing was determined using the N206 card on the Vitek 2 instrument (bioMérieux) calibrated against European Committee on Antimicrobial Susceptibility Testing (EUCAST) breakpoints. Minimum inhibitory concentrations (MICs) of meropenem, ertapenem, imipenem and colistin were determined using Etest (bioMérieux) for any isolate with reduced susceptibility to carbapenems on Vitek 2. Enterobacteriaceae with confirmed resistance to any carbapenem underwent further phenotypic testing using the KPC/MBL and OXA-48 Confirm kit (Rosco Diagnostica) to detect production of KPC, MBL and OXA-48 carbapenemases. All CPE (n=16) identified were de-duplicated for species and type of carbapenemase according to sample location, and further analysed using WGS (n=9).

Illumina sequencing and bioinformatic analyses

DNA extraction and library preparation were performed as previously described [23]. DNA libraries were sequenced using the Illumina HiSeq and MiSeq platforms (Illumina) to generate 100 and 150 bp paired-end reads, respectively. *De novo* multi-contig draft assemblies were generated using Velvet Optimiser and Velvet [24]. Contigs smaller than 300 bases were removed, the scaffolding software SSPACE was employed, and assemblies further improved using GapFiller. For isolates belonging to the *Enterobacter cloacae*complex, species identification was based on analysis of *hsp60* and *rpoB*, as described elsewhere [25]. To detect acquired genes encoding antimicrobial resistance, a manually curated version of the ResFinder database (compiled in 2012) [26] was used. Assembled sequences were compared to this as described previously [27], and genes with 100% match to length and >90% identity match were classified as present and variants identified. To establish genetic relatedness between *Raoultella ornithinolytica* isolates, Illumina sequence reads were mapped to the reference genome B6 (GenBank accession no. CP004142) using SMALT v0.7.4 to identify single-nucleotide polymorphisms (SNPs). SNPs were filtered to remove those at sites with a SNP quality score below 30, and SNPs at sites with heterogeneous mappings were filtered out if the SNP was present in less than 75% of reads at that site. Sequence data have been deposited in the European Nucleotide Archive (www.ebi.ac.uk/ena) under the individual accession numbers given in Table 1.

MinION sequencing and bioinformatic analyses

Isolates were streaked from frozen stock onto blood agar plates and incubated in air at 37 °C overnight. A sweep of colonies was taken and DNA extraction carried out using the QiaAMP DNA mini kit (Qiagen) and quantified using the Qubit fluorometer and BR kit (Life Technologies). Genomic DNA was diluted in 10 mM Tris-HCl to a concentration of 1500 ng in 46 µl and sheared using G-TUBES (Covaris). MinION sample preparation and two-dimensional sequencing was carried out as previously described using the SQK-MAP-006 kit and R7.3 flow cells [28]. Basecalling was carried out using the Metrichor two-dimensional basecalling option using version 1.15.7 for VRES0269 and VRES0273, and version 1.20.5 for VRES0259.

Basecalled MinION reads were converted from FAST5 to FASTQ and FASTA formats using fast52fastq.py (https://github.com/kim-judge/wastewater). Read mapping was carried out to assess the quality of data and coverage using the BWA-MEM algorithm of BWA v0.7.12 with the flag –x ont2d [29]. Output SAM files from BWA-MEM were converted to sorted BAM files using SAMtools v0.1.19-44428 cd [30]. Assembly using MinION data only was undertaken using Canu [31, 32], followed by Circlator [33] 1.2.0. Canu version 1.0 was run using the commands maxThreads=8, maxMemory=16, useGrid=0, nanopore-raw. Hybrid assemblies were generated using SPAdes 3.6 [34] using the –nanopore and –careful flags, then filtered to exclude contigs of less than 1 kb. All plasmid sequences and the chromosomes were confirmed to be circular by the Circlator software 1.2.0. Assembly statistics were analysed using assembly-stats (https://github.com/sanger-pathogens/assembly-stats). All assemblies were annotated using Prokka 1.5 [35, 36]. Assemblies were compared using the Artemis comparison tool [37] and further analysed using Artemis [38]. Plasmid sequences and other regions of interest were investigated using the BLASTN suite at National Center for Biotechnology Information (http://www.ncbi.nlm.nih.gov).

Manually finished genome

Assemblies were generated using Canu and SPAdes as described above. A gap5 database was made using corrected MinION pass reads from the Canu pipeline and the Illumina reads. Manual finishing was undertaken using gap5 [39] version 1.2.14 making one chromosome and nine plasmids. Icorn2 [40] was run on this for five iterations. The start positions of the chromosome and plasmids were fixed using Circlator [33] 1.2.0 using the command circlator fixstart. This assembly was annotated using Prokka 1.5 [35, 36].

Regional surveillance of CPE

Information was retrieved on all CPE isolates referred from diagnostic microbiology laboratories in the East of England to Public Health England's Antimicrobial Resistance and Healthcare Associated Infections (AMRHAI) Reference Unit between 2006 and 2015 (Table S1, available in the online Supplementary Material). KPC-, OXA-48-like-, NDM-, VIM- and IMP-encoding genes were detected by in-house PCR and/or commercial microarray, which was performed by the AMRHAI Reference Unit using published methods [41–46].

Go to:

Results

Isolation of CPE from wastewater

We undertook a cross-sectional study of 20 municipal wastewater treatment plants in the East of England between June 2014 and January 2015. Plant location was selected with reference to hospital waste, with ten plants situated immediately downstream of acute NHS Hospital Trust facilities (approximate median distance

between wastewater treatment plant and respective hospital 5.3 km, range 3.3–9.6 km) and ten plants not connected to acute hospital effluent (Fig. 1). Paired samples of untreated and treated wastewater were obtained from each plant. The main septic tank at the CUH facility was also sampled in September 2014. CPE were isolated using filtration and culture procedures (see Methods).

Fig. 1.

Map of wastewater treatment plants in the East of England tested for CPE. Black dots, negative for CPE; red dots, positive for CPE. Plants positive for CPE are numbered 1–4. Sewer refers to sampling at the CUH facility. Hospitals situated upstream of the study wastewater treatment plants (approximate median distance of 5.3 km; range 3.3–9.6 km) are denoted by H.

CPE were isolated from four plants and the CUH sewer (see Fig. 1 for locations). All four positive plants directly received hospital effluent. A total of nine bacterial isolates belonging to six species were cultured, all of which may cause human infection (Table 1). *E. coli* (*n*=1) and *R. ornithinolytica* (*n*=1) were isolated from treated water that was destined for release into the environment, and *Klebsiella pneumoniae* (*n*=3), *Klebsiella oxytoca* (*n*=1), *Enterobacter cloacae* complex (*n*=2) and *R. ornithinolytica* (*n*=1) were isolated from untreated water. In one case, the same species (*R. ornithinolytica*) was isolated from pre- and post-treated water sampled from the same plant.

Phenotypic evaluation of antimicrobial resistance

To characterize the carbapenemases in the nine isolates, we first used a phenotypic method that detects the three main biochemical groups of carbapenemases in Enterobacteriaceae. This identified a class A serine carbapenemase in *K. pneumoniae*, class B metallo-β-lactamases (MβLs) in *E. coli*, *K. pneumoniae* and *Enterobacter cloacae* complex, and class D OXA-48-like carbapenemases in *Enterobacter cloacae*complex, *K. pneumoniae*, *K. oxytoca* and the two *R. ornithinolytica* (Table 1). Susceptibility testing was conducted against a panel of antimicrobials, and demonstrated that all nine isolates were resistant to at least five antibiotic drug groups (Table 2).

Table 2.

Antimicrobial susceptibility of CPE isolated from wastewater

COL, Colistin; ETP, ertapenem; IPM, imipenem; MEM, meropenem; NI, non-identifiable by VITEK.

Red shading, resistant; blue shading, intermediate resistance; white/no shading, susceptible.

Comparison between wastewater findings and geographically related clinical isolates

To compare our findings with carbapenem-resistance mechanisms present in isolates cultured in the clinical setting in the same region, we collated data gathered by Public Health England on all CPE isolates referred by 16 diagnostic microbiology laboratories in the East of England to their AMRHAI Reference Unit for further characterization between 2006 and 2015. This identified 115 CPE isolates belonging to nine different Enterobacteriaceae species and harbouring carbapenemases belonging to classes A, B and D (Table S1). *K. pneumoniae*, *Escherichia coli* and members of the *Enterobacter cloacae* complex accounted for 43, 38 and 8% of isolates, respectively. The same bacterial species and carbapenemase gene (NDM) was observed in 2 wastewater treatment plants (numbered 1 and 2, Fig. 2) located downstream of hospitals where such CPEs were also identified.

Fig. 2.

CPE isolates referred from diagnostic microbiology laboratories in the East of England to the AMRHAI Reference Unit between 2008 and 2015. One representative of the same CPE per month per hospital is shown. One sample received by PHE in 2006 was excluded as date of isolation was unknown. See Table S1 for a complete list of all isolates.

Genetic characterization of antimicrobial resistance

The entire repertoire of resistance genes/mechanisms was characterized in the nine study isolates by performing WGS using Illumina short-read technology, followed by comparison of each genome to a comprehensive database of genes/gene variants that encode drug resistance (See Methods for details). From this, we identified carbapenemases in class A (GES-5), class B [NDM-5, NDM-1-like (differed from NDM-1 by 1 aa change) and IMP-1] and class D (OXA-48 and OXA-181) (Table 1), which are known to be carried by mobile genetic elements. Three isolates with high imipenem resistance also had truncated versions of porin proteins due to insertion sequences, stop mutations and frameshift mutations identified in ompC and ompF genes (Table 1). Disruption of these genes have been associated previously with high levels of carbapenem resistance [47]. Genes conferring resistance to multiple classes of antimicrobials were identified in all nine isolates, with gentamicin, quinolone and sulphonamide resistance being the most prevalent (Table 1).

Three CPE isolates were recovered from the same treatment plant: *Enterobacter cloacae* complex VRES0273 and *R. ornithinolytica* VRES0269 from pre-treated water, and *R. ornithinolytica* VRES0259 from post-treated water. VRES0273 was identified as *Enterobacter kobei* based on analysis of *hsp60* and *rpoB*, as described elsewhere [25, 48]. To assess the core genetic relatedness of the two *R. ornithinolytica*isolates, we aligned Illumina reads from both against the reference genome *R. ornithinolytica* B6 [49]. This identified that both genomes were over

18000 SNPs different from the reference over a core genome length of 5398151 bp (equating to 99.7% identity), but only 13 SNPs different between each other. This indicates a very high degree of relatedness. In addition, both *R. ornithinolytica* isolates had identical antibiotic-resistance patterns for 14/15 antimicrobials tested (Table 2). The three CPE isolates from this plant all contained the *bla*$_{OXA-48}$ gene conferring carbapenem resistance and the same non-β-lactam-resistance genes (Table 1).

Sharing of resistance plasmids between Enterobacteriaceae in wastewater

We hypothesized that resistance was mediated by one or more plasmids that were shared between these three isolates. We first examined the Illumina data alone to determine whether a plasmid carrying the *bla*$_{OXA-48}$ gene was the same in the three isolates, but predictably we failed to assemble complete plasmid sequence from this short-read data. From this, we were unable to conclude whether plasmids were shared, nor their specific content. The *bla*$_{OXA-48}$ gene was located on contigs of 2.5 kb (VRES273), 3.6 kb (VRES269) and 3.4 kb (VRES259) in the Illumina assemblies. To overcome this, DNA from the three isolates was sequenced using the MinION system to generate long-read data and assembled as described in Methods. From this we assembled a manually finished genome sequence for *Enterobacter kobei*(VRES0273), which represents the first complete whole-genome sequence for this species, and high-quality draft assemblies for the two *R. ornithinolytica* isolates. Tables 3 and S2 summarize the Illumina and MinION sequencing data. Using these assemblies, we were able to confirm the close genetic relationship between the two *R. ornithinolytica* isolates by mapping each against the other. These were 12 SNPs different over 5344247 aligned bases in a chromosome of 5462249 bp (VRES0269) and 5334936 aligned bases in a chromosome of 5392238 bp (VRES0259), corresponding to 99.9% identity in both cases, and covering 97.8 and 98.9% of the genome, respectively. One large genomic difference was present between the two isolates due to the absence of one of the four phages in VRES0259 (Fig. 3).

Fig. 3.

Comparison of whole-genome assemblies of *Enterobacter kobei* and *R. ornithinolytica* isolates using the Artemis comparison tool. The grey and dark blue vertical blocks represent BLAST hits between the isolates in the same orientation or in the inverted orientation, respectively. Only hits longer than 1 kb are shown. Contigs are highlighted in alternating orange and brown colours. The MDR plasmid is highlighted in light blue, and the *bla*$_{OXA-48}$ plasmid is highlighted in purple.

Table 3.

Assembly statistics for the nine CPE isolates based on Illumina and MinION data

Isolate ID	Species	Accession no.	Coverage	No. of contigs	Genome size [bp]	N50 [bp]*	Illumina or MinION data
VRES0316	*E. coli*	ERR885454	91×	104	5123602	197358	Illumina
VRES0375	*K. pneumoniae*	ERR885458	72×	114	6264863	220223	Illumina
VRES0377	*Enterobacter cloacae*complex	ERR1100748	72×	64	5499401	293804	Illumina
VRES0379	*K. oxytoca*	ERR1100749	52×	112	6676582	186596	Illumina
VRES0380	*K. pneumoniae*	ERR885459	88×	57	5657356	430982	Illumina
VRES0269	*R. ornithinolytica*	ERR885453	73×	99	6178860	235729	Illumina
		ERR1341571 ERR1341570	35×	14	6270467	3218273	MinION
		NA	NA	9	6345266	5614685	Both
VRES0273	*Enterobacter kobei*	ERR885455	75×	90	5454767	153115	Illumina

Isolate ID	Species	Accession no.	Coverage	No. of contigs	Genome size [bp]	N50 [bp]*	Illumina or MinION data
		ERR1341575 ERR1341574	42×	15	5542520	2782732	MinION
		NA	NA	13	5576147	5303011	Both
VRES0259	*R. ornithinolytica*	ERR1539195	654×	79	6179725	293454	Illumina
		ERR1341573 ERR1341572	65×	NA†	NA†	NA†	MinION
		NA	NA	19	6399880	1238878	Both
VRES0183	*K. pneumoniae*	ERR885457	80×	68	5544688	300916	Illumina

Open in a separate window

NA, Not applicable.

*N50 is a weighted median statistic. Half (50%) of the assembly is contained in contigs greater than or equal to a contig of this size.

†There is no MinION only assembly for VRES0259 as the data for this isolate was only sufficient to make a hybrid assembly.

One contig from each isolate (74 kb in *Enterobacter kobei*, 69 kb in *R. ornithinolytica* VRES259 and 63 kb in *R. ornithinolytica* VRES269) contained the bla_{OXA-48} gene (Fig. 4a). Based on BLAST searches and assembly comparisons using the Artemis comparison tool, these contigs showed synteny and orthology to other widespread IncL/M-type bla_{OXA-48} plasmids in *Enterobacter cloacae, R. ornithinolytica* and *K. pneumoniae* (GenBank

examples: JN626286.1, KP061858.1, NC_023027.1, CVRH01000036 to CVRH01000038 and LN864819.1) [41, 50–54]. The plasmids from the three isolates were identical to each other over a shared region of 63 kb, with zero SNPs difference. Variation in overall size was due to hypothetical proteins integrated via insertion sequence (IS) elements. There were several transposases, which were located around the *bla*$_{OXA-48}$ gene and forming part of the Tn*1999* transposon (Fig. 4a). Similar variation in plasmids encoding other carbapenemases has been identified in isolates from different species at a single hospital [9, 10].

Fig. 4.

Comparison of shared *Enterobacter kobei* and *R. ornithinolytica* plasmids. (a) *bla*$_{OXA-48}$ pOXA-48a-like plasmid. (b) Multidrug-resistance plasmid. Plasmid maps of the shared plasmids are shown, with genes of interest annotated. The grey and blue blocks represent BLAST hits between the isolates in the same orientation and inverted orientation, respectively. The colour intensity is proportional to the per cent identity of the match, within the specific region. Gene colour code indicates function: dark blue, heavy-metal resistance; light blue, conjugational transfer; dark pink, antibiotic resistance; light pink, IS elements and transposases; yellow, replication, maintenance, partitioning genes; light green, other (hypothetical proteins, host metabolism, regulators and pseudogenes).

We also identified a 297 kb contig in *Enterobacter kobei*, a 318 kb contig in *R. ornithinolytica* VRES259 and a 281 kb contig in *R. ornithinolytica* VRES269 from long-read data (Fig. 3). All three contigs were identified as an IncHI2 type plasmid using *in silico* PCR [55]. These carried heavy-metal-resistance genes for mercury, tellurium and arsenic, and conjugational transfer genes that facilitate plasmid transfer between different species of Enterobacteriaceae (Fig. 3b). A multidrug-resistance region similar to those found in *Enterobacter cloacae* [56] (GenBank examples: CP012170.1, EU855788.1, CP008899.1) was also identified in this plasmid, which contained resistance genes for aminoglycosides [(aac(6′)-*IIc*, aac(6′)-*Ib*), ethidium bromide (*emrE*), rifampicin (*arr2*), quinolones (*qnrA1*), sulphonamides (*sul1*, *sul2*) and third-generation cephalosporins (*bla*$_{SHV-12}$)]. This multidrug-resistance region was flanked by transposases, indicating the potential for excision and horizontal gene transfer (Fig. 4b). The shared plasmid had a common 280 kb region, which contained three SNPs between the *Enterobacter kobei* plasmid and the other two plasmids, and zero SNPs between the *R. ornithinolytica* plasmids.

Go to:

Discussion

To our knowledge, this is the first report of CPE being recovered from wastewater at UK sewage treatment plants. Our demonstration of the co-circulation of a diversity of pathogenic, carbapenem-resistant Gram-negative species carrying different resistance genes in sewage confirms that this is a complex and diverse reservoir. We also confirmed that treatment processes do not prevent the release of CPE into the environment, which will contribute to contamination of river and

lakes, farmland, vegetable land and fisheries, with the potential for spread to humans and livestock. Human infection caused by bacteria such as those identified here would prove challenging to treat with available antimicrobial drugs.

All CPE isolates were recovered from plants located downstream of hospitals. The same bacterial species and carbapenemase gene (encoding NDM) was found in two hospitals and the downstream wastewater treatment plant, indicating that the resistance mechanisms found in wastewater are likely to mirror those associated with human disease. Currently, no national regulation nor the European Directive 91/271/EEC on urban wastewater treatment stipulates the use of disinfection of hospital wastewater in the UK, and as a result this may be contributing to the dissemination of CPE [57, 58]. Further studies are required to fully ascertain the role of hospital effluent as a source of environmental contamination with CPE.

Phenotypic methods presumptively identify the presence of the most common CPEs (KPC, MBL, OXA-48), but are unable to identify variant types. We used genome sequencing to identify variants of carbapenemase-resistance genes, to detect sequence alterations in porin genes associated with decreased membrane permeability (an important factor contributing to carbapenem resistance [59]), and to define the full repertoire of resistance genes. The use of long-read sequencing data enabled us to conclude that two Enterobacteriaceae species (*R. ornithinolytica* and *Enterobacter kobei*) in treated and untreated wastewater carried highly similar plasmids containing numerous genes encoding resistance to antimicrobials and heavy metals. Whilst the rate of mutation in plasmids may vary from that of the chromosome, our findings are consistent with the suggestion that a globally distributed bla_{OXA-48} plasmid was shared very recently between the two species (0 SNPs different), a figure that is contextualized by comparison with a published sequence of plasmid pOXA-48a [50], which was more than 100 SNPs different. This plasmid is known to be the origin of the widespread dissemination of bla_{OXA-48} and, similar to our findings, has a broad bacterial host range and does not encode additional antimicrobial-resistance genes [50, 60]. In addition, a recent report from Findlay *et al.* in 2017 [3] identified OXA-48-like enzymes as being the second most frequently detected carbapenemases in the West Midlands region of the UK between 2007 and 2014 based on a study of 119 clinical isolates, including one environmental isolate from an endoscope camera head in a urology theatre. OXA-48-like enzymes were identified in 16/119 isolates from three different bacterial species (*K. pneumoniae*, *E. coli* and *Citrobacterfreundii*). Similar to the plasmids detected in our study, five IncL/M plasmids were identified using WGS, which exhibited >99% identity to pOXA-48a with no additional resistance genes. These genome data were not publicly available and no genome comparison was possible with our data, but based on similarity to pOXA-48a and genetic content we postulate that a highly related plasmid encoding bla_{OXA-48} is found in both UK wastewater and associated with human infection. Similar to pOXA-48a, the bla_{OXA-48} gene and the transposases identified in our study are part of the Tn*1999* transposon, indicating the mobility of this gene independent of the plasmid backbone (Fig. 4a). It has also been shown in an early characterization of this plasmid that it is highly identical and syntenic to the pCTX-M3 plasmid, except for the Tn*1999* transposon from which it might have evolved [50].

The multidrug and heavy-metal resistance plasmid was highly similar in both species, although this acquisition may have occurred less recently based on a three SNP difference between the *R. ornithinolytica*and the *Enterobacter kobei* plasmid. Based on the published mutation rate for *K. pneumoniae* (2.7×10^{-6} SNPs per site per year, equating to 14 SNPs per genome per year) [61], this would suggest that the plasmids last shared a common ancestor more than 3 years ago. Identification of such resistance plasmids spreading within and between bacterial species is essential when trying to understand the epidemiology of CPE, as has been shown in studies using PacBio sequencing [9, 10]. A study by Sheppard *et al.* [10] particularly emphasizes that a similar detailed picture of plasmid transfer and variability is not available when only studying short-read data, which may prove misleading.

The main limitation of this study is the lack of quantification of CPE load per sample. This was due to technical limitations relating to the incomplete selectivity of currently available CPE media (which results in overgrowth of organisms other than CPE), combined with the low prevalence of CPE in samples. This leads to a low positive predictive value for detection of a true CPE from the growth obtained on the plate and makes quantitation extremely challenging. In order to enrich for low numbers of CPE in a very high bacterial background, we used an additional selective enrichment step (tryptic soy broth with imipenem), which increased the yield of CPE, but ruled out quantitation. Furthermore, the study was conducted in a region with very low CPE prevalence and may not be generalizable across the UK [62]. Future studies including longitudinal data from additional regions and hospitals will provide further insights into the community spread of CPE.

In conclusion, the combined use of Illumina and MinION technologies revealed sharing of plasmids carrying multiple antimicrobial-resistance genes between different bacterial species in wastewater, including the plasmid encoding OXA-48 that confers carbapenem resistance. Whilst phenotypic testing resolved the general class of carbapenemase and short-read data identified the specific carbapenemase genes involved, long-read data was essential to resolve the plasmid architecture and for accurate comparisons. Small, portable sequencing instruments, such as the MinION, have the potential for use in real-time genomic surveillance in a One Health approach that includes genetic material from wastewater, animals and hospitals to monitor the effectiveness of treatment systems, and to contribute to the development of interventions to limit the dissemination of antimicrobial resistance.

Go to:

Data bibliography

1. Ludden C, Reuter S, Judge K, Gouliouris T, Blane B *et al.* European Nucleotide Archive, ERS634376 and ERS1033541 (MinION sequence data) (2017).

2. Ludden C, Reuter S, Judge K, Gouliouris T, Blane B *et al.* Github. https://github.com/kim-judge/wastewater (2017).

3. Judge K, Hunt M, Reuter S, Tracey A, Quail, MA *et al.* European Nucleotide Archive, ERS634378 (MinION sequence data) (2016).

4. Judge K, Hunt M, Reuter S, Tracey A, Quail, MA *et al.* European Nucleotide Archive, ERS634378: FKLS01000001-FKLS01000010 (2016).

Go to:

Funding information

This publication presents independent research supported by the Health Innovation Challenge Fund (WT098600, HICF-T5-342), a parallel funding partnership between the Department of Health, UK, and the Wellcome Trust. The views expressed in this publication are those of the author(s) and not necessarily those of the Department of Health nor the Wellcome Trust. C. L. is a Wellcome Trust Sir Henry Postdoctoral Fellow (110243/Z/15/Z). T. G. is a Wellcome Trust Research Training Fellow (103387/Z/13/Z).

Go to:

Acknowledgements

We gratefully acknowledge the contribution of the staff at the waste- water treatment plants for assistance in sample collection. We are grateful for assistance with Illumina sequencing from the library construction, sequencing and core informatics teams at the Wellcome Trust Sanger Institute. We thank Simon Harris for advice on assembling long-read data, Mike Quail for sequencing support, and the staff at Oxford Nanopore for their technical support and advice during the MinION Access Program.

Go to:

Conflicts of interest

K. J. is a member of the MinION Access Program and received free-of-charge reagents for the MinION sequencing presented in this study. All other authors have no conflicts to declare.

Go to:

Ethical statement

The study was approved by the National Research Ethics Service (reference: 14/EE/1123) and Cambridge University Hospitals NHS Foundation Trust Research and Development Department (reference: A093285).

References

1. Nordmann P, Naas T, Poirel L. Global spread of carbapenemase-producing *Enterobacteriaceae*. Emerg Infect Dis. 2011;17:1791–1798. doi: 10.3201/eid1710.110655. [PMC free article] [PubMed] [CrossRef] [Google Scholar]
2. Jain A, Hopkins KL, Turton J, Doumith M, Hill R, et al. NDM carbapenemases in the United Kingdom: an analysis of the first 250 cases. J Antimicrob Chemother. 2014;69:1777–1784. doi: 10.1093/jac/dku084.[PubMed] [CrossRef] [Google Scholar]
3. Findlay J, Hopkins KL, Alvarez-Buylla A, Meunier D, Mustafa N, et al. Characterization of carbapenemase-producing Enterobacteriaceae in the West Midlands region of England: 2007–14. J Antimicrob Chemother. 2017;72::1054–1062. doi: 10.1093/jac/dkw560. [PubMed] [CrossRef] [Google Scholar]
4. Woodford N, Wareham DW, Guerra B, Teale C. Carbapenemase-producing Enterobacteriaceae and non-Enterobacteriaceae from animals and the environment: an emerging public health risk of our own making? J Antimicrob Chemother. 2014;69:287–291. doi: 10.1093/jac/dkt392. [PubMed] [CrossRef] [Google Scholar]
5. Tzouvelekis LS, Markogiannakis A, Piperaki E, Souli M, Daikos GL. Treating infections caused by carbapenemase-producing *Enterobacteriaceae*. Clin Microbiol Infect. 2014;20:862–872. doi: 10.1111/1469-0691.12697. [PubMed] [CrossRef] [Google Scholar]
6. Falagas ME, Tansarli GS, Karageorgopoulos DE, Vardakas KZ. Deaths attributable to carbapenem-resistant *Enterobacteriaceae* infections. Emerg Infect Dis. 2014;20:1170–1175. doi: 10.3201/eid2007.121004. [PMC free article] [PubMed] [CrossRef] [Google Scholar]
7. Wellington EM, Boxall AB, Cross P, Feil EJ, Gaze WH, et al. The role of the natural environment in the emergence of antibiotic resistance in Gram-negative bacteria. Lancet Infect Dis. 2013;13:155–165. doi: 10.1016/S1473-3099(12)70317-1. [PubMed] [CrossRef] [Google Scholar]
8. Haller S, Eller C, Hermes J, Kaase M, Steglich M, et al. What caused the outbreak of ESBL-producing *Klebsiella pneumoniae* in a neonatal intensive care unit, Germany 2009 to 2012? Reconstructing transmission with epidemiological analysis and whole-genome sequencing. BMJ Open. 2015;5:e007397. doi: 10.1136/bmjopen-2014-007397. [PMC free article] [PubMed] [CrossRef] [Google Scholar]
9. Conlan S, Thomas PJ, Deming C, Park M, Lau AF, et al. Single-molecule sequencing to track plasmid diversity of hospital-associated carbapenemase-producing Enterobacteriaceae. Sci Transl Med. 2014;6:254ra126. doi: 10.1126/scitranslmed.3009845. [PMC free article] [PubMed] [CrossRef] [Google Scholar]
10. Sheppard AE, Stoesser N, Wilson DJ, Sebra R, Kasarskis A, et al. Nested Russian doll-like genetic mobility drives rapid dissemination of the carbapenem resistance gene bla_{KPC}. Antimicrob Agents Chemother. 2016;60:3767–3778. doi: 10.1128/AAC.00464-16. [PMC free article] [PubMed] [CrossRef] [Google Scholar]
11. Judge K, Harris SR, Reuter S, Parkhill J, Peacock SJ. Early insights into the potential of the Oxford Nanopore MinION for the detection of antimicrobial

resistance genes. J Antimicrob Chemother. 2015;70:2775–2778. doi: 10.1093/jac/dkv206. [PMC free article] [PubMed] [CrossRef] [Google Scholar]
12. Ashton PM, Nair S, Dallman T, Rubino S, Rabsch W, et al. MinION nanopore sequencing identifies the position and structure of a bacterial antibiotic resistance island. Nat Biotechnol. 2015;33:296–300. doi: 10.1038/nbt.3103. [PubMed] [CrossRef] [Google Scholar]
13. Quick J, Loman NJ, Duraffour S, Simpson JT, Severi E, et al. Real-time, portable genome sequencing for Ebola surveillance. Nature. 2016;530:228–232. doi: 10.1038/nature16996. [PMC free article] [PubMed] [CrossRef] [Google Scholar]
14. Turton JF, Doumith M, Hopkins KL, Perry C, Meunier D, et al. Clonal expansion of *Escherichia coli*ST38 carrying a chromosomally integrated OXA-48 carbapenemase gene. J Med Microbiol. 2016;65:538–546. doi: 10.1099/jmm.0.000248. [PubMed] [CrossRef] [Google Scholar]
15. Oliveira S, Moura RA, Silva KC, Pavez M, Mcculloch JA, et al. Isolation of KPC-2-producing *Klebsiella pneumoniae* strains belonging to the high-risk multiresistant clonal complex 11 (ST437 and ST340) in urban rivers. J Antimicrob Chemother. 2014;69:849–852. doi: 10.1093/jac/dkt431. [PubMed] [CrossRef] [Google Scholar]
16. Isozumi R, Yoshimatsu K, Yamashiro T, Hasebe F, Nguyen BM, et al. bla_{NDM-1}-positive *Klebsiella pneumoniae* from environment, Vietnam. Emerg Infect Dis. 2012;18:1383–1385. doi: 10.3201/eid1808.111816. [PMC free article] [PubMed] [CrossRef] [Google Scholar]
17. Montezzi LF, Campana EH, Corrêa LL, Justo LH, Paschoal RP, et al. Occurrence of carbapenemase-producing bacteria in coastal recreational waters. Int J Antimicrob Agents. 2015;45:174–177. doi: 10.1016/j.ijantimicag.2014.10.016. [PubMed] [CrossRef] [Google Scholar]
18. Zurfluh K, Hächler H, Nüesch-Inderbinen M, Stephan R. Characteristics of extended-spectrum β-lactamase- and carbapenemase-producing *Enterobacteriaceae* isolates from rivers and lakes in Switzerland. Appl Environ Microbiol. 2013;79:3021–3026. doi: 10.1128/AEM.00054-13.[PMC free article] [PubMed] [CrossRef] [Google Scholar]
19. Poirel L, Barbosa-Vasconcelos A, Simões RR, da Costa PM, Liu W, et al. Environmental KPC-producing *Escherichia coli* isolates in Portugal. Antimicrob Agents Chemother. 2012;56:1662–1663. doi: 10.1128/AAC.05850-11. [PMC free article] [PubMed] [CrossRef] [Google Scholar]
20. Galler H, Feierl G, Petternel C, Reinthaler FF, Haas D, et al. KPC-2 and OXA-48 carbapenemase-harbouring Enterobacteriaceae detected in an Austrian wastewater treatment plant. Clin Microbiol Infect. 2014;20:O132–O134. doi: 10.1111/1469-0691.12336. [PubMed] [CrossRef] [Google Scholar]
21. Girlich D, Poirel L, Szczepanowski R, Schlüter A, Nordmann P. Carbapenem-hydrolyzing GES-5-encoding gene on different plasmid types recovered from a bacterial community in a sewage treatment plant. Appl Environ Microbiol. 2012;78:1292–1295. doi: 10.1128/AEM.06841-11. [PMC free article][PubMed] [CrossRef] [Google Scholar]
22. Picão RC, Cardoso JP, Campana EH, Nicoletti AG, Petrolini FVB, et al. The route of antimicrobial resistance from the hospital effluent to the environment: focus on the occurrence of KPC-producing *Aeromonas* spp. and

Enterobacteriaceae in sewage. Diagn Microbiol Infect Dis. 2013;76:80–85. doi: 10.1016/j.diagmicrobio.2013.02.001. [PubMed] [CrossRef] [Google Scholar]
23. Köser CU, Holden MT, Ellington MJ, Cartwright EJ, Brown NM, et al. Rapid whole-genome sequencing for investigation of a neonatal MRSA outbreak. N Engl J Med. 2012;366:2267–2275. doi: 10.1056/NEJMoa1109910. [PMC free article] [PubMed] [CrossRef] [Google Scholar]
24. Zerbino DR, Birney E. Velvet: algorithms for de novo short read assembly using de Bruijn graphs. Genome Res. 2008;18:821–829. doi: 10.1101/gr.074492.107. [PMC free article] [PubMed] [CrossRef] [Google Scholar]
25. Hoffmann H, Roggenkamp A. Population genetics of the nomenspecies *Enterobacter cloacae*. Appl Environ Microbiol. 2003;69:5306–5318. doi: 10.1128/AEM.69.9.5306-5318.2003. [PMC free article][PubMed] [CrossRef] [Google Scholar]
26. Zankari E, Hasman H, Cosentino S, Vestergaard M, Rasmussen S, et al. Identification of acquired antimicrobial resistance genes. J Antimicrob Chemother. 2012;67:2640–2644. doi: 10.1093/jac/dks261.[PMC free article] [PubMed] [CrossRef] [Google Scholar]
27. Reuter S, Ellington MJ, Cartwright EJ, Köser CU, Török ME, et al. Rapid bacterial whole-genome sequencing to enhance diagnostic and public health microbiology. JAMA Intern Med. 2013;173:1397–1404. doi: 10.1001/jamainternmed.2013.7734. [PMC free article] [PubMed] [CrossRef] [Google Scholar]
28. Judge K, Hunt M, Reuter S, Tracey A, Quail MA, et al. Comparison of bacterial genome assembly software for MinION data and their applicability to medical microbiology. Microb Genom. 2016;2:e000085. doi: 10.1099/mgen.0.000085. [PMC free article] [PubMed] [CrossRef] [Google Scholar]
29. Li H, Durbin R. Fast and accurate short read alignment with Burrows-Wheeler transform. Bioinformatics. 2009;25:1754–1760. doi: 10.1093/bioinformatics/btp324. [PMC free article] [PubMed] [CrossRef] [Google Scholar]
30. Li H, Handsaker B, Wysoker A, Fennell T, Ruan J, et al. The sequence alignment/map format and SAMtools. Bioinformatics. 2009;25:2078–2079. doi: 10.1093/bioinformatics/btp352. [PMC free article][PubMed] [CrossRef] [Google Scholar]
31. Berlin K, Koren S, Chin CS, Drake JP, Landolin JM, et al. Assembling large genomes with single-molecule sequencing and locality-sensitive hashing. Nat Biotechnol. 2015;33:623–630. doi: 10.1038/nbt.3238. [PubMed] [CrossRef] [Google Scholar]
32. Koren S, Walenz BP, Berlin K, Miller JR, Bergman NH, et al. Canu: scalable and accurate long-read assembly via adaptive *k*-mer weighting and repeat separation. Genome Res. 2017;27:722–736. doi: 10.1101/gr.215087.116. [PMC free article] [PubMed] [CrossRef] [Google Scholar]
33. Hunt M, Silva ND, Otto TD, Parkhill J, Keane JA, et al. Circlator: automated circularization of genome assemblies using long sequencing reads. Genome Biol. 2015;16:294. doi: 10.1186/s13059-015-0849-0.[PMC free article] [PubMed] [CrossRef] [Google Scholar]

34. Bankevich A, Nurk S, Antipov D, Gurevich AA, Dvorkin M, et al. SPAdes: a new genome assembly algorithm and its applications to single-cell sequencing. J Comput Biol. 2012;19:455–477. doi: 10.1089/cmb.2012.0021. [PMC free article] [PubMed] [CrossRef] [Google Scholar]
35. Seemann T. Prokka: rapid prokaryotic genome annotation. Bioinformatics. 2014;30:2068–2069. doi: 10.1093/bioinformatics/btu153. [PubMed] [CrossRef] [Google Scholar]
36. Page AJ, de Silva N, Hunt M, Quail MA, Parkhill J, et al. Robust high-throughput prokaryote de novo assembly and improvement pipeline for Illumina data. Microb Genom. 2016;2::e000083. doi: 10.1099/mgen.0.000083. [PMC free article] [PubMed] [CrossRef] [Google Scholar]
37. Carver TJ, Rutherford KM, Berriman M, Rajandream MA, Barrell BG, et al. ACT: the Artemis comparison tool. Bioinformatics. 2005;21:3422–3423. doi: 10.1093/bioinformatics/bti553. [PubMed] [CrossRef] [Google Scholar]
38. Rutherford K, Parkhill J, Crook J, Horsnell T, Rice P, et al. Artemis: sequence visualization and annotation. Bioinformatics. 2000;16:944–945. doi: 10.1093/bioinformatics/16.10.944. [PubMed] [CrossRef] [Google Scholar]
39. Bonfield JK, Whitwham A. Gap5—editing the billion fragment sequence assembly. Bioinformatics. 2010;26:1699–1703. doi: 10.1093/bioinformatics/btq268. [PMC free article] [PubMed] [CrossRef] [Google Scholar]
40. Otto TD, Sanders M, Berriman M, Newbold C. Iterative Correction of Reference Nucleotides (iCORN) using second generation sequencing technology. Bioinformatics. 2010;26:1704–1707. doi: 10.1093/bioinformatics/btq269. [PMC free article] [PubMed] [CrossRef] [Google Scholar]
41. Poirel L, Héritier C, Tolün V, Nordmann P. Emergence of oxacillinase-mediated resistance to imipenem in *Klebsiella pneumoniae*. Antimicrob Agents Chemother. 2004;48:15–22. doi: 10.1128/AAC.48.1.15-22.2004. [PMC free article] [PubMed] [CrossRef] [Google Scholar]
42. Ellington MJ, Kistler J, Livermore DM, Woodford N. Multiplex PCR for rapid detection of genes encoding acquired metallo-β-lactamases. J Antimicrob Chemother. 2007;59:321–322. doi: 10.1093/jac/dkl481. [PubMed] [CrossRef] [Google Scholar]
43. Mushtaq S, Irfan S, Sarma JB, Doumith M, Pike R, et al. Phylogenetic diversity of *Escherichia coli*strains producing NDM-type carbapenemases. J Antimicrob Chemother. 2011;66:2002–2005. doi: 10.1093/jac/dkr226. [PubMed] [CrossRef] [Google Scholar]
44. Yigit H, Queenan AM, Anderson GJ, Domenech-Sanchez A, Biddle JW, et al. Novel carbapenem-hydrolyzing β-lactamase, KPC-1, from a carbapenem-resistant strain of *Klebsiella pneumoniae*. Antimicrob Agents Chemother. 2001;45:1151–1161. doi: 10.1128/AAC.45.4.1151-1161.2001.[PMC free article] [PubMed] [CrossRef] [Google Scholar]
45. Woodford N, Warner M, Pike R, Zhang J. Evaluation of a commercial microarray to detect carbapenemase-producing Enterobacteriaceae. J Antimicrob Chemother. 2011;66:2887–2888. doi: 10.1093/jac/dkr374. [PubMed] [CrossRef] [Google Scholar]

46. Ellington MJ, Findlay J, Hopkins KL, Meunier D, Alvarez-Buylla A, et al. Multicentre evaluation of a real-time PCR assay to detect genes encoding clinically relevant carbapenemases in cultured bacteria. Int J Antimicrob Agents. 2016;47:151–154. doi: 10.1016/j.ijantimicag.2015.11.013. [PubMed] [CrossRef] [Google Scholar]
47. Doumith M, Ellington MJ, Livermore DM, Woodford N. Molecular mechanisms disrupting porin expression in ertapenem-resistant *Klebsiella* and *Enterobacter* spp. clinical isolates from the UK. J Antimicrob Chemother. 2009;63:659–667. doi: 10.1093/jac/dkp029. [PubMed] [CrossRef] [Google Scholar]
48. Zhou K, Yu W, Bonnet R, Cattoir V, Shen P, et al. Emergence of a novel *Enterobacter kobei* clone carrying chromosomal-encoded CTX-M-12 with diversified pathogenicity in northeast China. New Microbes New Infect. 2017;17:7–10. doi: 10.1016/j.nmni.2017.01.006. [PMC free article] [PubMed] [CrossRef] [Google Scholar]
49. Shin SH, Um Y, Beak JH, Kim S, Lee S, et al. Complete genome sequence of *Raoultella ornithinolytica* strain B6, a 2,3-butanediol-producing bacterium isolated from oil-contaminated soil. Genome Announc. 2013;1:e00395-13. doi: 10.1128/genomeA.00395-13. [PMC free article] [PubMed] [CrossRef] [Google Scholar]
50. Poirel L, Bonnin RA, Nordmann P. Genetic features of the widespread plasmid coding for the carbapenemase OXA-48. Antimicrob Agents Chemother. 2012;56:559–562. doi: 10.1128/AAC.05289-11.[PMC free article] [PubMed] [CrossRef] [Google Scholar]
51. Poirel L, Potron A, Nordmann P. OXA-48-like carbapenemases: the phantom menace. J Antimicrob Chemother. 2012;67:1597–1606. doi: 10.1093/jac/dks121. [PubMed] [CrossRef] [Google Scholar]
52. Manageiro V, Pinto M, Caniça M. Complete sequence of a bla_{OXA-48}-harboring IncL plasmid from an *Enterobacter cloacae* clinical isolate. Genome Announc. 2015;3:e01076-15. doi: 10.1128/genomeA.01076-15. [PMC free article] [PubMed] [CrossRef] [Google Scholar]
53. Power K, Wang J, Karczmarczyk M, Crowley B, Cotter M, et al. Molecular analysis of OXA-48-carrying conjugative IncL/M-like plasmids in clinical isolates of *Klebsiella pneumoniae* in Ireland. Microb Drug Resist. 2014;20:270–274. doi: 10.1089/mdr.2013.0022. [PubMed] [CrossRef] [Google Scholar]
54. Al-Bayssari C, Olaitan AO, Leangapichart T, Okdah L, Dabboussi F, et al. Whole-genome sequence of a bla_{OXA-48}-harboring *Raoultella ornithinolytica* clinical isolate from Lebanon. Antimicrob Agents Chemother. 2016;60:2548–2550. doi: 10.1128/AAC.02773-15. [PMC free article] [PubMed] [CrossRef] [Google Scholar]
55. Carattoli A, Bertini A, Villa L, Falbo V, Hopkins KL, et al. Identification of plasmids by PCR-based replicon typing. J Microbiol Methods. 2005;63:219–228. doi: 10.1016/j.mimet.2005.03.018. [PubMed] [CrossRef] [Google Scholar]
56. Chen YT, Liao TL, Liu YM, Lauderdale TL, Yan JJ, et al. Mobilization of *qnrB2* and IS*CR1* in plasmids. Antimicrob Agents Chemother. 2009;53:1235–1237. doi: 10.1128/AAC.00970-08.[PMC free article] [PubMed] [CrossRef] [Google Scholar]

57. Water UK. London:: Water UK;; 2014. *National Guidance for Healthcare Waste Water Discharges*; issue date August 2014.https://dldropboxusercontentcom/u/299993612/Publications/Guidance/Waste water/Water[Google Scholar]
58. Hocquet D, Muller A, Bertrand X. What happens in hospitals does not stay in hospitals: antibiotic-resistant bacteria in hospital wastewater systems. J Hosp Infect. 2016;93:395–402. doi: 10.1016/j.jhin.2016.01.010. [PubMed] [CrossRef] [Google Scholar]
59. Uz Zaman T, Aldrees M, Al Johani SM, Alrodayyan M, Aldughashem FA, et al. Multi-drug carbapenem-resistant *Klebsiella pneumoniae* infection carrying the OXA-48 gene and showing variations in outer membrane protein 36 causing an outbreak in a tertiary care hospital in Riyadh, Saudi Arabia. Int J Infect Dis. 2014;28:186–192. doi: 10.1016/j.ijid.2014.05.021. [PubMed] [CrossRef] [Google Scholar]
60. Carattoli A, Seiffert SN, Schwendener S, Perreten V, Endimiani A. Differentiation of IncL and IncM plasmids associated with the spread of clinically relevant antimicrobial resistance. PLoS One. 2015;10:e0123063. doi: 10.1371/journal.pone.0123063. [PMC free article] [PubMed] [CrossRef] [Google Scholar]
61. Chung The H, Karkey A, Pham Thanh D, Boinett CJ, Cain AK, et al. A high-resolution genomic analysis of multidrug-resistant hospital outbreaks of *Klebsiella pneumoniae*. EMBO Mol Med. 2015;7:227–239. doi: 10.15252/emmm.201404767. [PMC free article] [PubMed] [CrossRef] [Google Scholar]
62. Trepanier P, Mallard K, Meunier D, Pike R, Brown D, et al. Carbapenemase-producing Enterobacteriaceae in the UK: a national study (EuSCAPE-UK) on prevalence, incidence, laboratory detection methods and infection control measures. J Antimicrob Chemother. 2017;72:596–603. doi: 10.1093/jac/dkw414. [PubMed] [CrossRef] [Google Scholar]